

# Safe Buffers around Einstein Telescope Corner Points

Shahar Shani-Kadmiel | RDSA | KNMI

18 September 2021

---

## Summary

Wind turbines<sup>1</sup> emit seismic signals due to the rotation of the blades and the movement of the tower. Seismic signals radiated from wind turbines are known to interfere with operational seismic monitoring of natural and induced seismicity. With regard to the Einstein Telescope and the design of the passive and active vibration isolation systems, the seismic radiation from wind turbines poses a major challenge.

We deployed seismic sensors to the west of the Aachen wind park and analyzed the power spectral density (PSD) at each station. Our analysis indicates that the amplitude of distinct spectral peaks decreases as a function of distance from the wind park. These spectral peaks are at 1.1, 2.2, and 3.2 Hz and can be attributed to the seismic signal emitted by the wind turbines in the Aachen wind park.

In Figure 1, we present the PSD of the noise measured during a temporary seismic campaign from December 14, 2020 to January 20, 2021. Each curve represents a noise measurement at a different station positioned at varying distances from the Aachen wind park. The spectral peaks associated with the wind turbines in the wind park are highlighted by vertical gray lines. The amplitude of these peaks decreases as a function of distance from the wind park. Furthermore, the amplitude of these peaks is correlated with the wind speed measured at the top of the wind turbines.

The seismic station TERZ in Terziet, hosts a sensor at the surface and a sensor at a depth of 250 meters below the surface. Seismic noise at the surface is generally attenuated with increasing depth, especially when soft, unconsolidated soil layers at the surface overlay hard rock layers. In TERZ, the top 40 m are relatively soft and below this point hard rocks are found. Therefore, at frequencies above about 1 Hz, where noise from anthropogenic activity becomes significant, the amplitude of the noise at 250 m depth is many orders of magnitude lower than at the surface. However, the spectral peaks associated with the wind turbines more than 13 km away are still visible.

---

<sup>1</sup> Apart from wind turbines, for example also major roads, railroads, heavy industry and mining activities can degrade the quality of a potential site to host the Einstein Telescope. These are not addressed in this note.

The assumption that the upper soil layer dampens noise from anthropogenic activity at the surface is correct, but for tall structures that are founded in the hard rock, this upper soil layer is of little significance. This applies for wind turbines in this region especially in the Belgian part of this area.

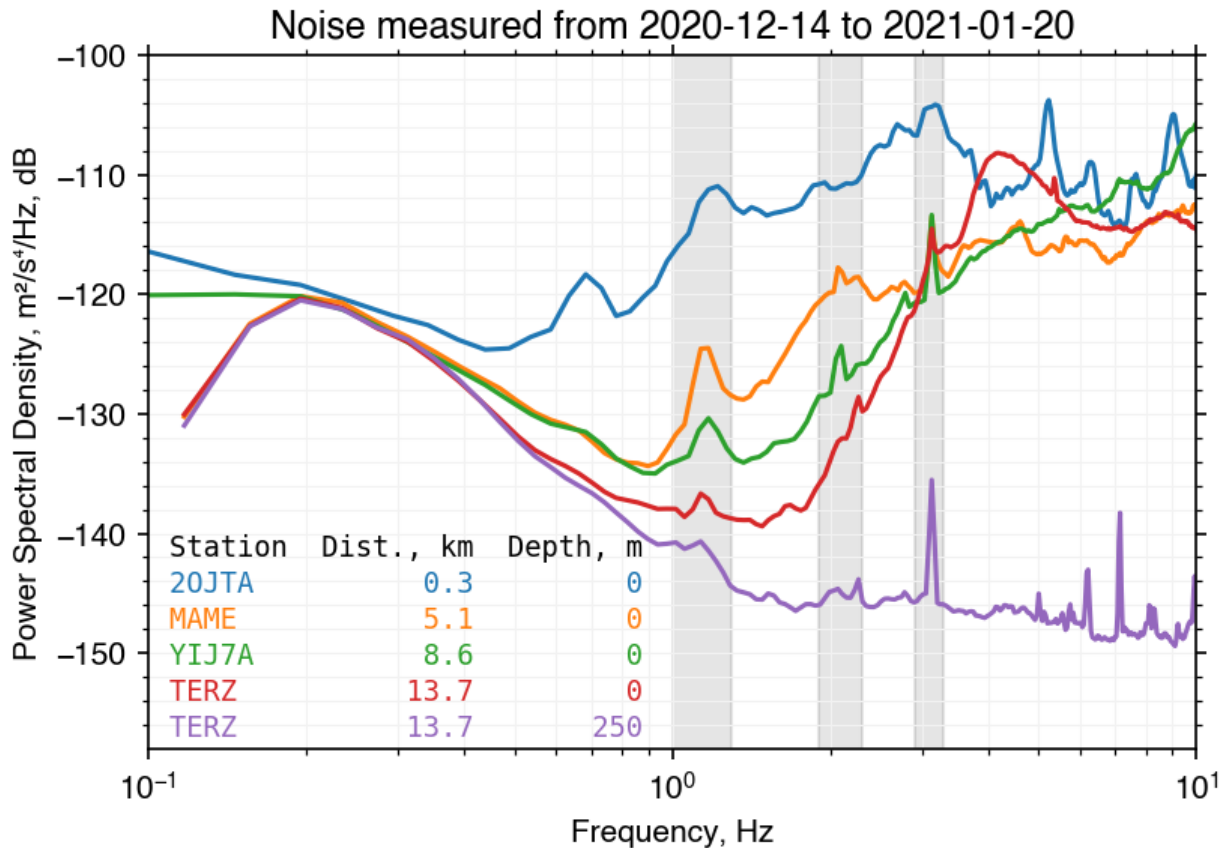


**Figure 1:** (PSD) Amplitude as a function of distance from the wind park. The 1.1, 2.2, & 3.2 Hz peaks, highlighted by vertical gray lines, are consistently decreasing as a function of distance from the wind park. The station name, distance from the wind park, and local depth of the sensor are indicated in the bottom-left corner. The color of the text corresponds to the color of the curve. The 7 Hz peak is most likely related to resonance in the steel pipe casing the borehole.

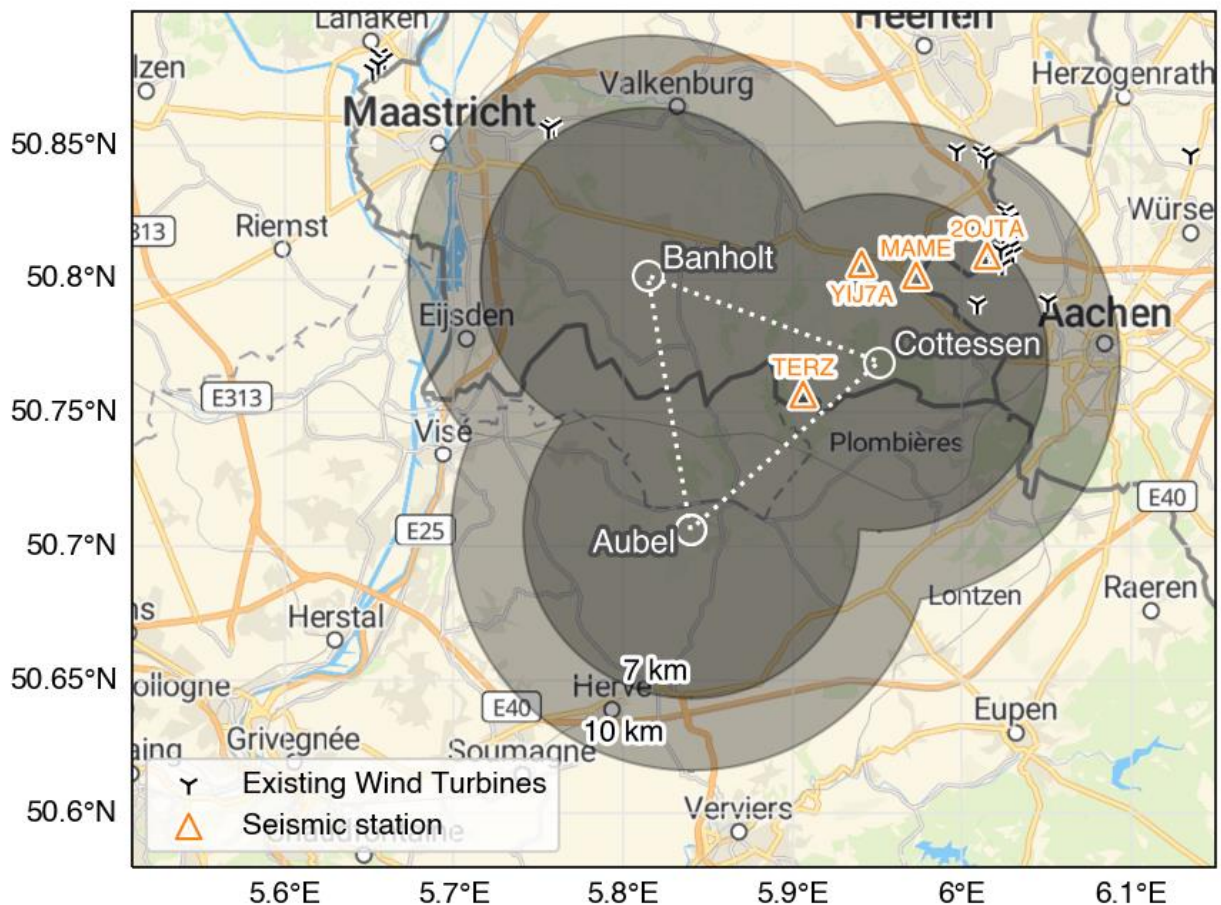
Using the results from the spectral analysis, we outline two buffer regions<sup>2</sup> around the sensitive corner points planned for the Einstein Telescope. In the first buffer region, out to 7 km, the construction of new wind turbines is extremely undesirable. In the second

<sup>2</sup> It should be noted that the effect of wind turbines on the performance of the Einstein Telescope does not solely depend on the distance; The height, foundation depth, rotational frequency of the blades, etc., also come into play.

buffer region, out to 10 km, the construction of new wind turbines might pose unwanted challenges and might affect the sensitivity of the detector.

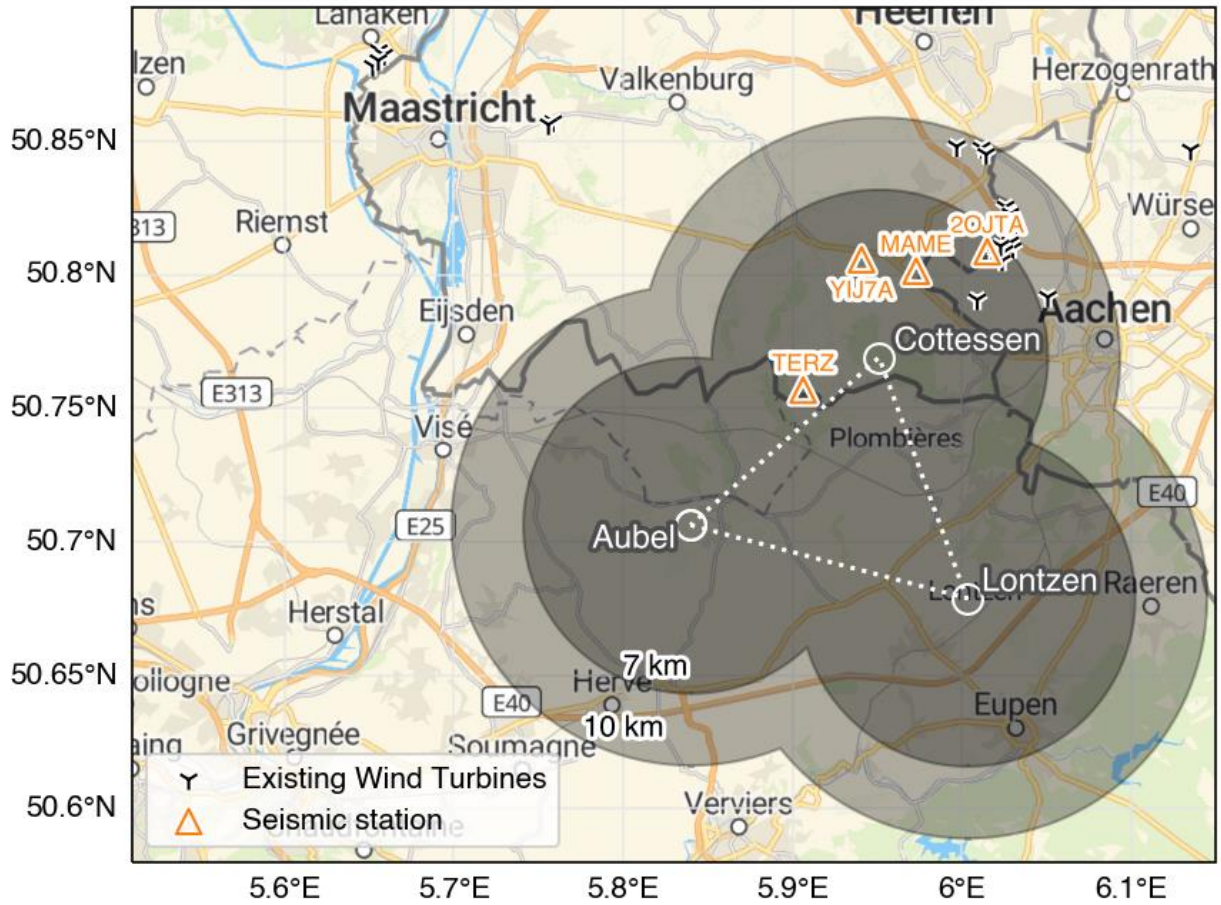
## Option A

The following map presents the two buffer regions around the Cottessen - Aubel - Banholt corner points, the location of the seismic sensors used in the spectral analysis above, and the location of existing wind turbines in the region. Due to noise the corner points will be situated well outside the villages or buildings and never constructed directly below habited zones. The name next to each corner point corresponds to the nearest village and is a rough indication in which region the corner points could be situated with regard to our current knowledge of the geology.



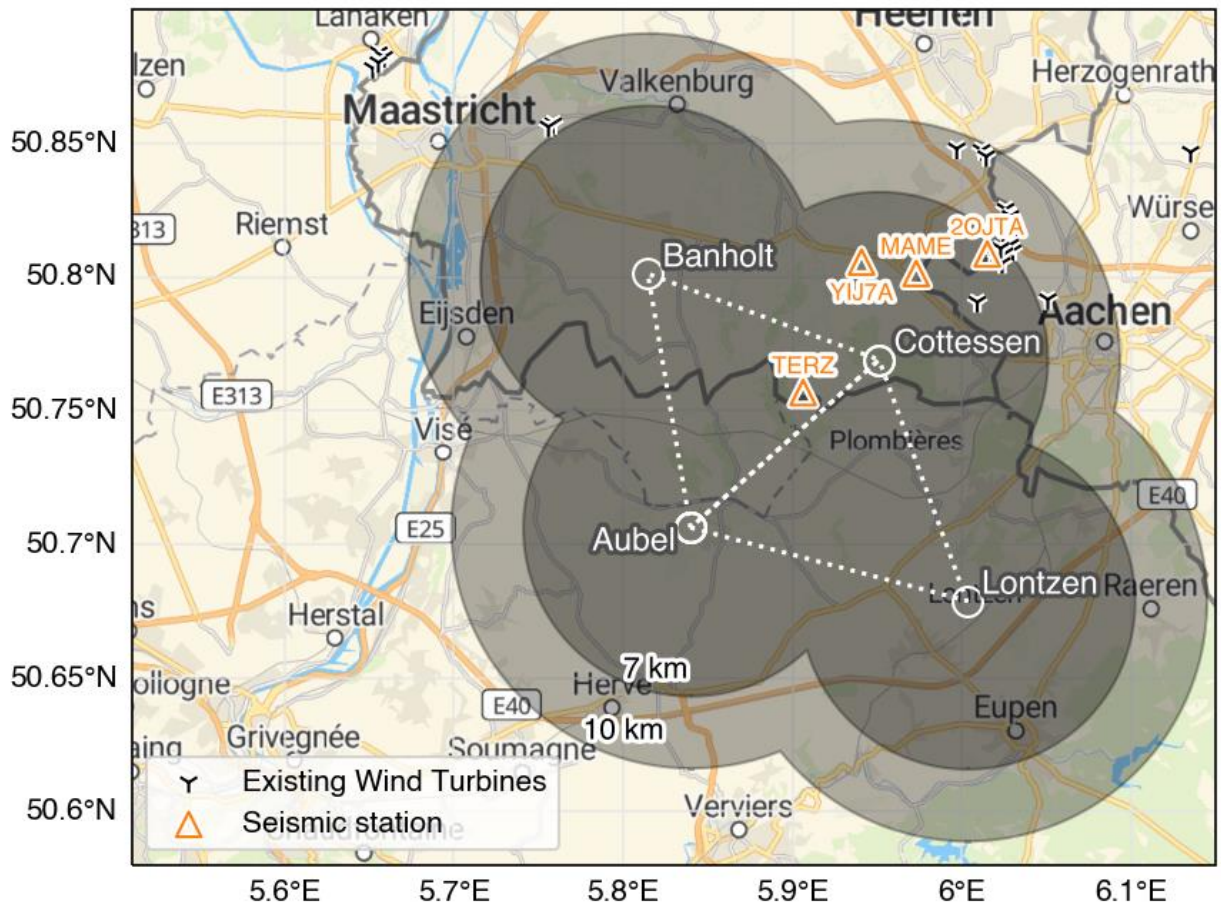
## Option B

The following map presents the two buffer regions around the Cottessen - Aubel - Lontzen corner points, the location of the seismic sensors used in the spectral analysis above, and the location of existing wind turbines in the region.



## Union of options A and B (A U B)

The following map presents the two buffer regions combined around the above two options.



# Wind Turbine Seismic Monitoring Campaign for ETEST

## Intermediate report

Shahar Shani-Kadmiel<sup>a</sup>, Bjorn Vink<sup>b</sup>, Frank Linde<sup>c</sup>

<sup>a</sup>*R&D Seismology and Acoustics, Royal Netherlands Meteorological Institute (KNMI),  
De Bilt, The Netherlands.*

<sup>b</sup>*Antea Group, Maastricht, The Netherlands.*

<sup>c</sup>*Gravitational-wave research, Nikhef, Amsterdam, The Netherlands.*

---

## Summary

Wind turbines emit seismic signals due to the rotation of the blades and the movement of the tower. Seismic signals radiated from wind turbines are known to interfere with operational seismic monitoring of natural and induced seismicity. With regard to the Einstein Telescope and the design of the passive and active vibration isolation systems, the seismic radiation from wind turbines poses a major challenge. The objective of this study is to characterize the radiated seismic field from the Aachen wind park in terms of amplitude, frequency, attenuation, the influence of wind speed and type of seismic waves.

We deployed 21 geophones west of the Aachen wind park and analyzed the power spectral density at each station. Our analysis indicates that the amplitude of distinct spectral peaks decreases as a function of distance from the wind park. Namely, these spectral peaks are 1.1, 2.2, and 3.2 Hz. Additionally, we found that the amplitude, of the entire spectrum, but specifically of the above spectral peaks is correlated with wind speed.

---

## Introduction

In this campaign, we deployed five mini-arrays west of the Aachen wind park (Figure 1) with the aim to characterize the radiated seismic field from wind turbines. This is one part of our effort to better understand sources of noise and the effect they might have on the Einstein Telescope, an advanced and super sensitive Gravitational-wave observatory, if it were to be built in the Euregio Meuse-Rhine region.

The motivation for deploying arrays, rather than single stations, is to in-addition to analyzing the power spectral density (PSD) at each station, beamform the wavefield and extract the direction to the various sources relative to each array. Discussion of the beamforming results are not differed to a later report.

---

\*with contributions from: Pooya Hamdi, Nina Engels, Shuyang Deng, Jonathan Zinser, Klaus Reicherter, Florian Amann, Soumen Koley, Láslo Evers

We deployed the sensors on December 14, 2020 and retrieved them on January 19, 2021. We chose this period to capture the ambient seismic field during the relatively quiet holiday period (Christmas and New Year's) and typically strong winds in the region. During this period, there were days with almost no wind and there were days with more than 20 m/s (90 km/h) wind. During this campaign there was also an active swarm of earthquakes unraveling in the vicinity of Rott, Germany, roughly 20 km south-east to our sensors (see Figure 1). These were well recorded by our sensors as-well-as by the seismic networks of the KNMI, and ROB.

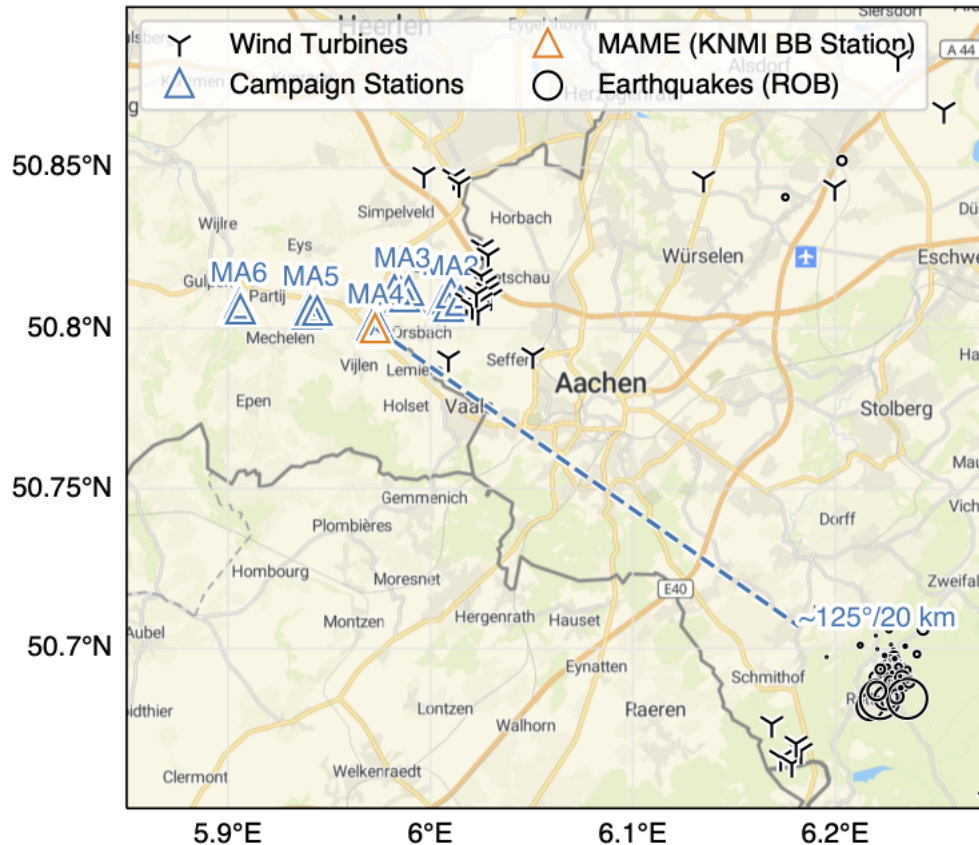


Figure 1: Overview map of the deployed mini-arrays (MA), the Aachen wind park, and the Rott earthquake swarm.

## Power Spectral Densities

Our PSD analysis indicates that the amplitude of distinct spectral peaks decreases as a function of distance from the wind park (Figure 2). Namely, these spectral peaks are 1.1, 2.2, and 3.2 Hz. This suggests that these spectral peaks are associated with the wind park. To further substantiate this, we analyzed PSD amplitudes as a function of wind speed. We found that the amplitude, of the entire spectrum, but specifically of the above spectral peaks is correlated with wind speed (Figure 3).

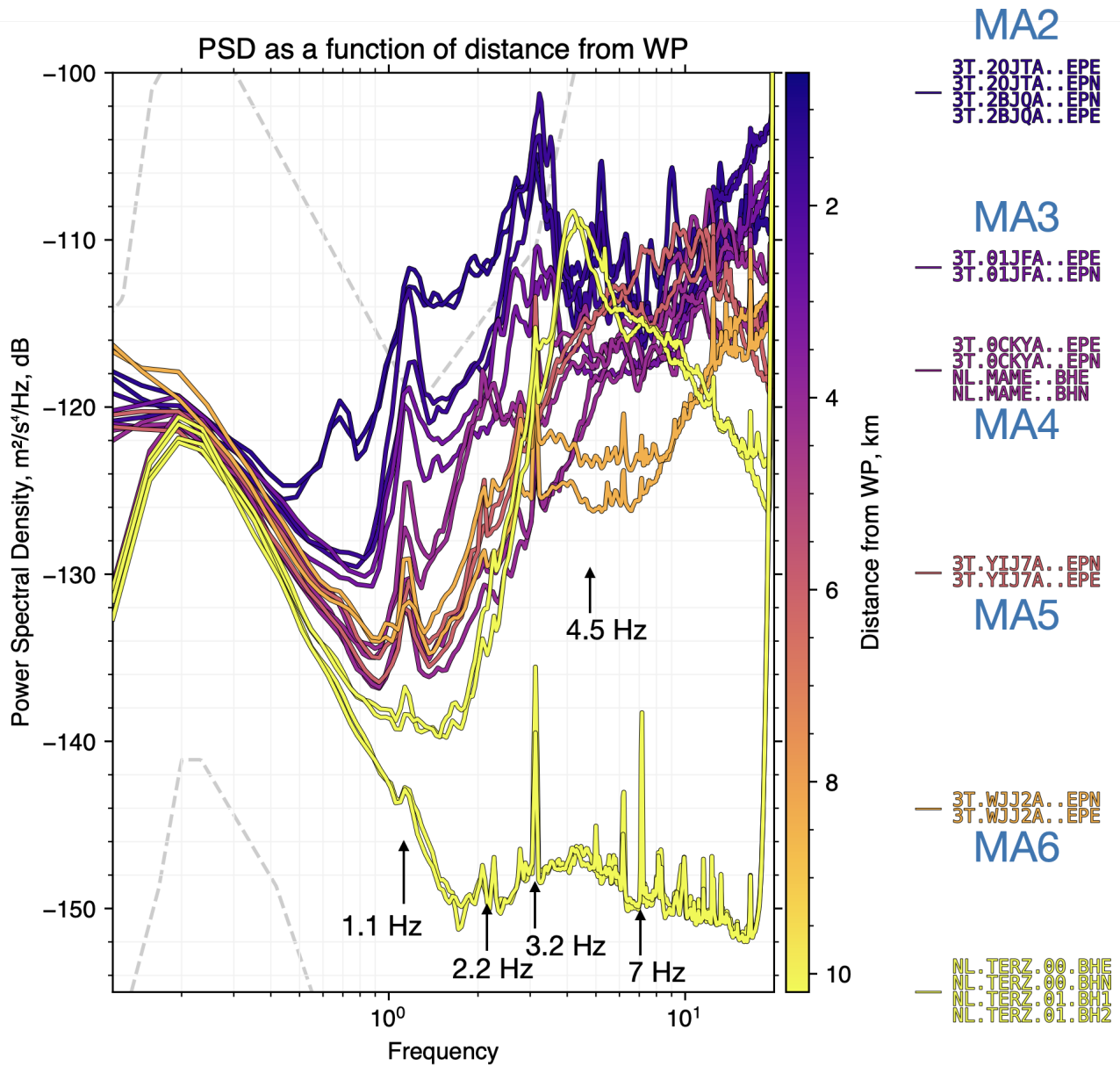


Figure 2: PSD as a function of distance from the wind park. The 1.1, 2.2, & 3.2 Hz peaks are consistently decreasing as a function of distance from the wind park. The yellow curves at just over 10 km distance from the wind park, were computed for station NL.TERZ, which hosts broadband seismometers at the surface and at 250 m deep in a steel cased borehole. The 4.5 Hz peak remains unexplained at this time and the 7 Hz peak, is most likely related to resonance in the steel casing.

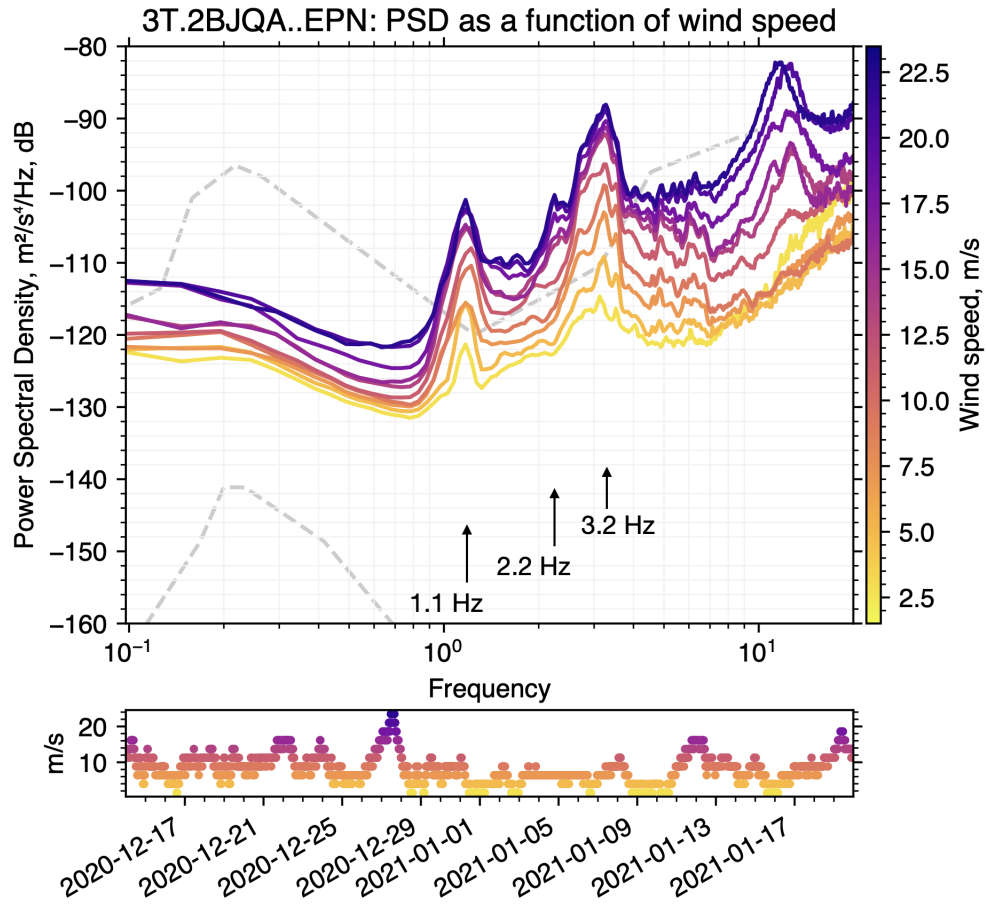


Figure 3: PSD as a function of wind speed at station 3T.2BJQA. The 1.1, 2.2, & 3.2 Hz peaks are consistently decreasing as a function of wind speed.

## Concluding remarks

- Spectral peaks of 1.1, 2.2, and 3.2 Hz have been clearly identified to be related to wind turbines. These change as a function of wind and as a function of distance from the wind park and are visible even at 250 m depth more than 10 km away.
- The assumption that the upper soil layer is a vibration insulator is correct for anthropogenic activity on the surface but fails when large structures are founded in the hard rock, or when the activity is in the hard rock itself.

Why is the entire spectrum affected by wind speed?

- At the surface: Probably due to wind interaction with the surface itself, trees, vegetation, and other structures.
- At depth: Probably due to structures founded in the hard rock.

# **Seismic Measurements at the Stateline Wind Project**

## **And A Prediction of the Seismic Signal that the Proposed Maiden Wind Project Would Produce at LIGO**

**Robert Schofield, Ph.D., University of Oregon**

### **Summary**

**Measurements of ground vibration were made at 10 sites around the Stateline Wind Project. The 3-bladed turbines produce seismic peaks mainly at multiples of 3 times their rotation frequency. The strongest peak (4.3 Hz) was detected at a site about 18 km from Stateline where it reached 0.7 nm/sqrt(Hz) of ground motion. Signal amplitudes were fit best with a  $1/r$  attenuation model, suggesting that the propagation path is partly through the air. The signal level that the Maiden project (both phases) would produce at the LIGO site (about 20 km distant) was estimated, with a high degree of uncertainty, to be about equal to the present background level at LIGO.**

**The accuracy of the predictions could be improved by measurements at a site that uses the turbines planned for the Maiden project. For example, it is possible that the rotation rate of the Maiden turbines would vary to a degree that the peaks from the individual turbines did not “pile up” as much at a particular frequency. Measurements at a site that employs the proposed Maiden turbines are recommended.**

### **Motivation**

The Laser Interferometric Gravitational wave Observatory (LIGO) on the Hanford reservation is concerned that the seismic signal from the Maiden wind project may shake precisely positioned mirrors. Perhaps the greatest danger to LIGO is that one (or more) of the potential peaks from the Maiden site match the frequency of a resonance in the seismic isolation system. An example of such an unlucky coincidence is a 2.3 Hz peak (from cooling tower fans at a nearby nuclear power plant) that exceeds the surrounding background at LIGO by only a factor of about 5. Because it matches a seismic isolation system resonance, this peak is responsible for about 20% of the r.m.s. of the frequency noise in one interferometer, prior to special servo modification. A similar amplitude signal from the Maiden Wind Project, at a resonance, could contribute much more to this r.m.s. because the peak would be wider. This could create a need for abatement modifications.

### **Measurements**

#### **Instrumentation**

Seismic measurements were made using a Guralp CMG-40T seismometer whose outputs were fed through a Stanford SR-560 preamplifier into an HP 3857 signal analyzer. Instruments were powered by internal or external (automobile) batteries. At sites 1 and 2, the seismometer was placed on a granite slab set directly on the earth at the bottom of a meter deep pit (Figure 1). The pit was walled and capped with a wooden box. The box top was then covered with a couple of inches of earth to bring the level up to the surrounding grade. At other sites, the seismometer was shielded from wind using an overturned plastic tub instead of a pit.



**Figure 1.** Seismometer in pit at site 2.

## Calibration

The instrumentation described above was set up, using identical instrument settings, near a LIGO seismometer. The signal level calculated from the HP 3857 output, using the manufacturer's calibration, matched the signal level output by the LIGO data system. Noise floors for each of the instrument settings used during data collection at the Stateline site were determined by replacing the seismometer with a resistor matched to the seismometer output resistance. Noise floors were below signal level for spectra shown here.

## Results

### *Measurement Locations*

Measurements were made at 10 locations. Seismometer pits were excavated at two sites. Site 1 was located 24 meters SW of the base of turbine HGJ-44 (Figure 2). Site 2 was located 1660 m (about 1 mile) from HGA-1 and is shown on the map of Figure 3. At the other locations, plastic tubs were used instead of pits. These locations were as follows: site 3, on the cement base of HGJ-44, site 4, 50 meters from HGA-1 (Fig. 3), site 5, 100 meters from HGA-1 on Hatch Grade Rd. (Fig. 3), site 6, 150 m from the base of HGA-1 at the corner of Hatch Grade and Braden Ranch roads (Fig. 3), site 7, located 710 m from HGA-1 on Hatch Grade road (Fig. 3), site 8, about 3 km from HGA-1, across the Walla Walla river (Fig. 4), site 9, about 11 km away on Dodd road (Fig. 4), and, site 10, about 18 km away in



**Figure 2.** Site 1: the pit was in the shadow of the mound at the lower left; the base of HGJ-44 is 24 m away in the near background

the McNary National Wildlife Refuge (Fig. 4).

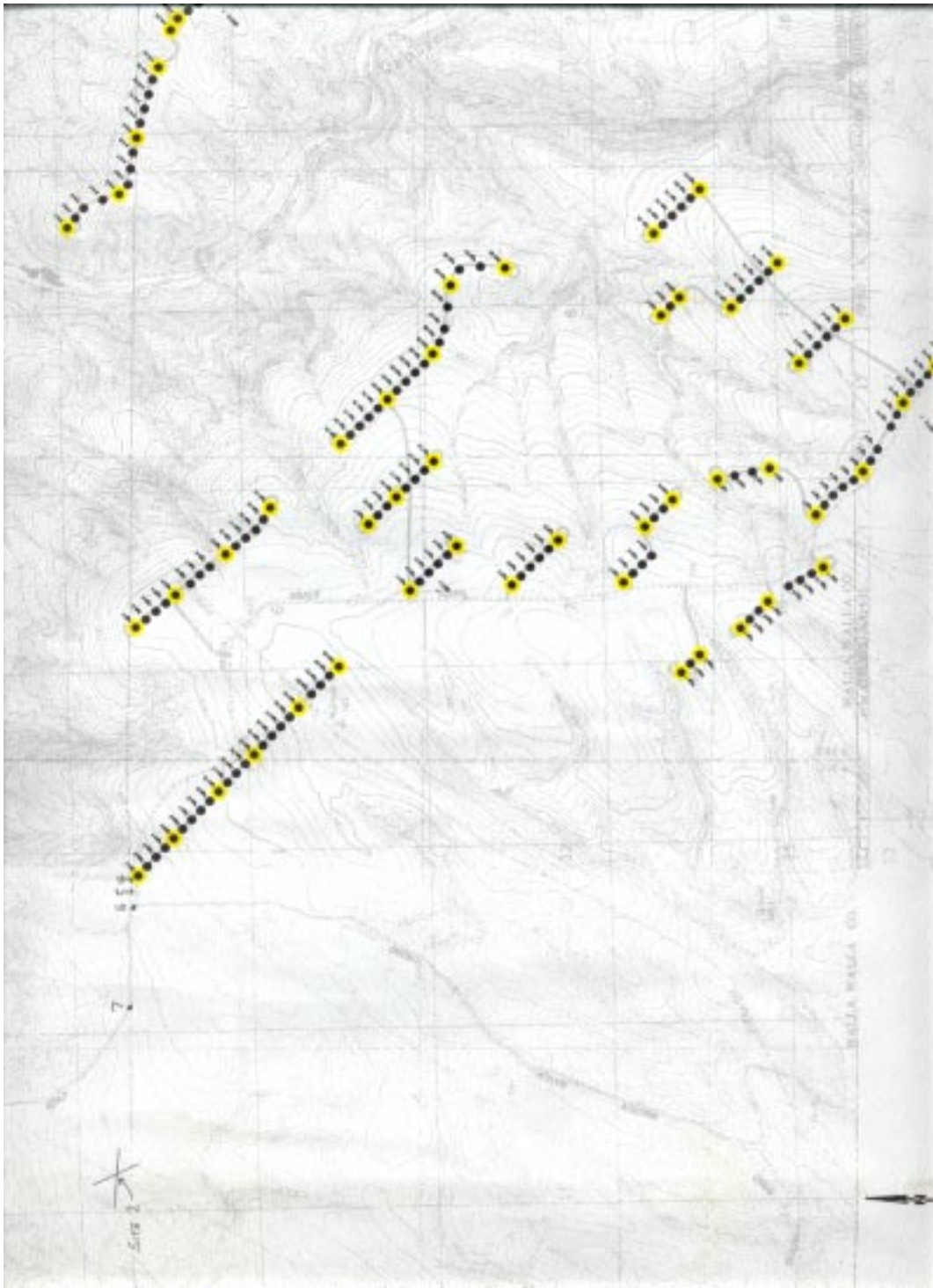


Figure 3



**Figure 4.**

### *Spectra*

Figures 5 and 6 show spectra from sites 1 and 2. The figures show a low frequency and a high frequency measurement for each site. The LIGO spectra were taken the same evening as the Maiden spectra; the wind speed at LIGO for this data averaged about 8 m/s.

### Vertical Motion at Sites 1 & 2

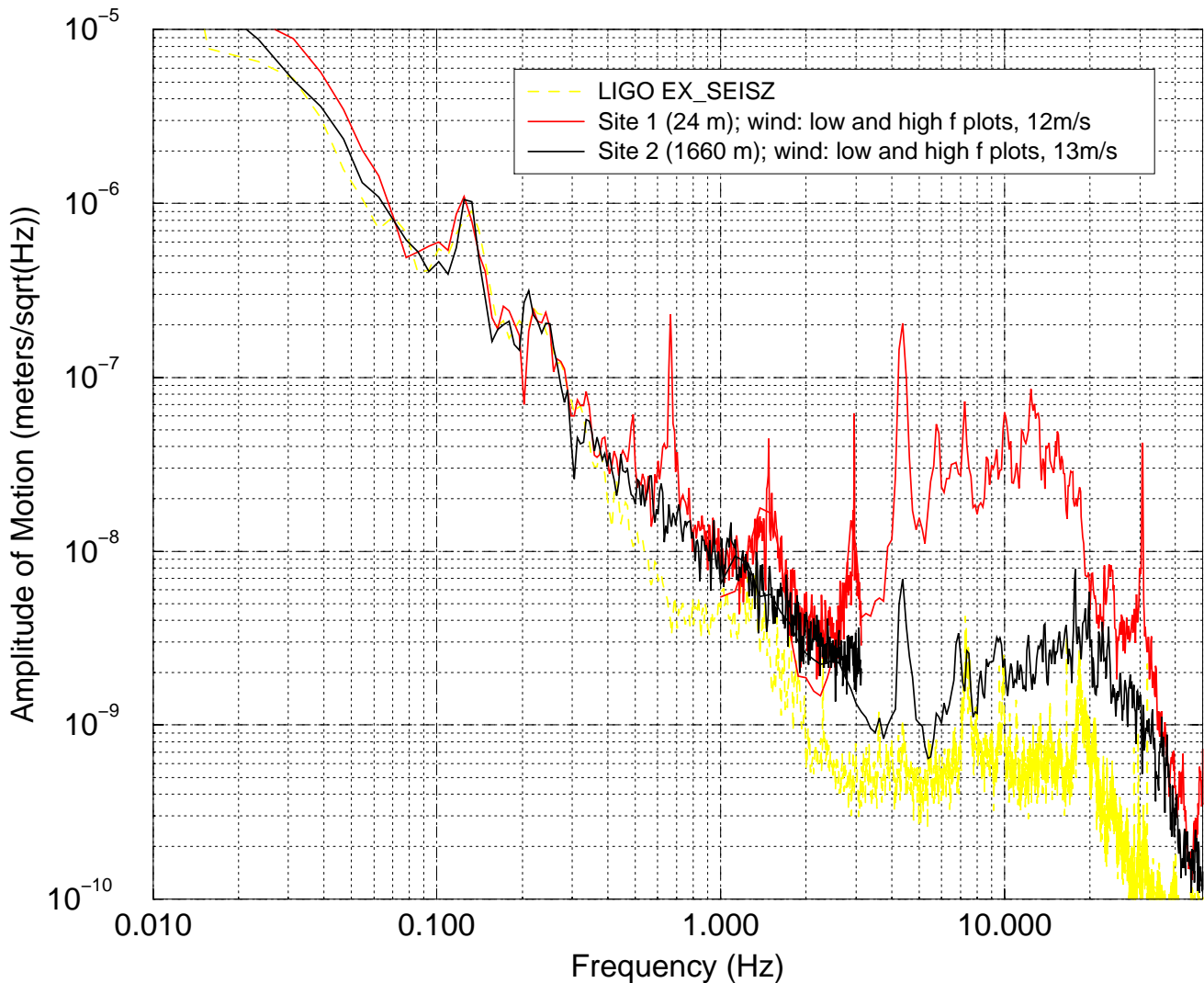
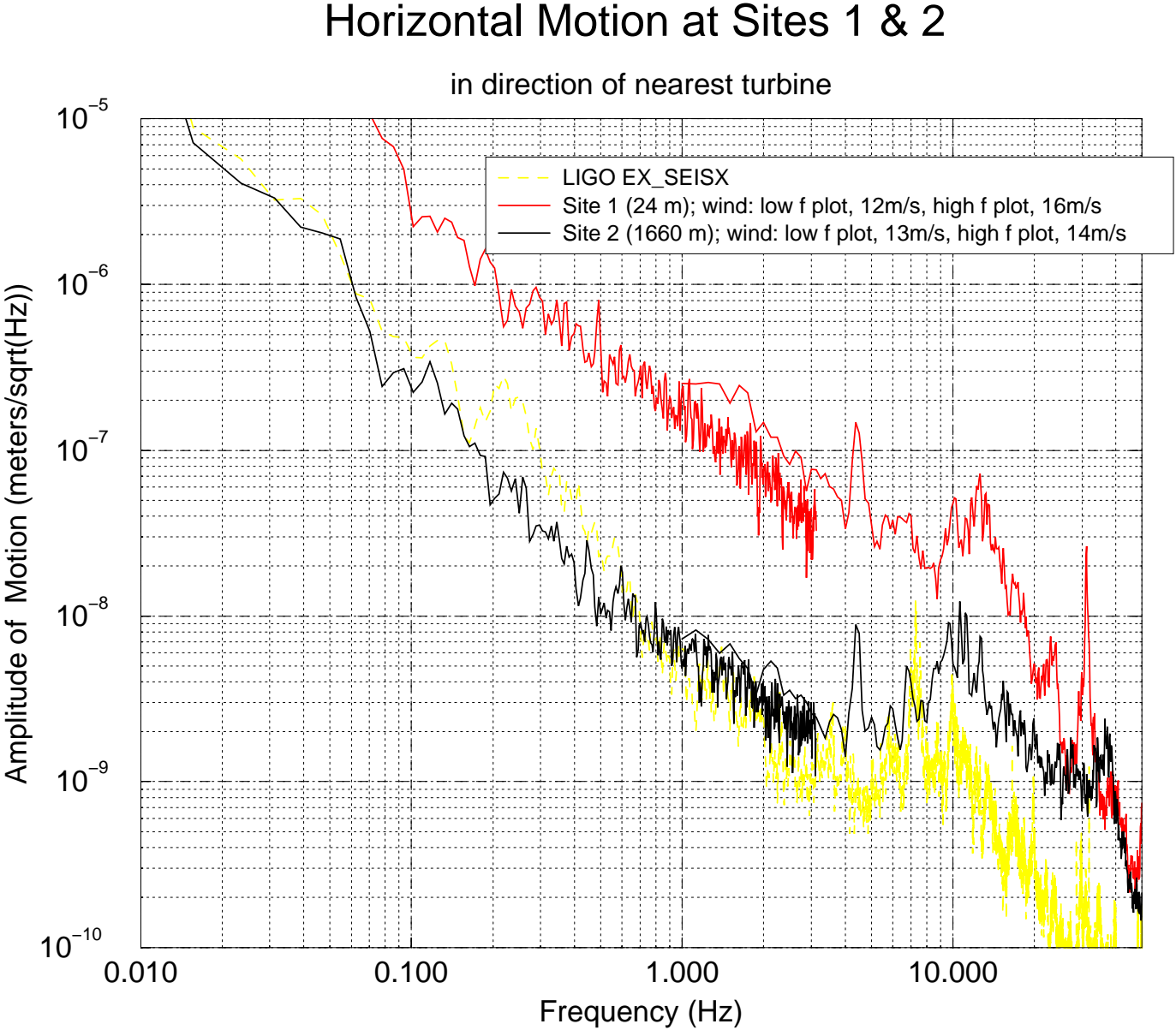


Figure 5.

Figure 6.



### *Signal Identification*

Signals were attributed to the turbines if they were relatively larger nearer to the base of the tower. Two types of peaks were identified, stationary frequency peaks, presumably associated with structural resonances, and peaks whose frequency varied with turbine rotation rate. To discriminate between these two types, a seismometer was set up on the base of a turbine tower (site 3) during a period of low wind velocity, when many turbines were not moving. The peaks identified below as stationary were observed at the same frequency as during high wind velocity periods. The peaks identified as varying were observed to increase in frequency as the rotation rate of the turbine increased. At higher wind velocities these varying frequencies stabilize because the turbine is designed to run at a nearly constant rotation rate (OptiSlip-equipped induction generators allow about a 10% variation in rate).

**Table 1: Peaks that decreased in frequency at low wind velocities**

Approximate frequency at high wind velocity (Hz)	Comments
0.49	rotation frequency of turbine (29 rpm)
1.47	3rd harmonic of rotation frequency (blade pass frequency)
2.95	6th harmonic
4.34	9th harmonic (largest peak relative to background)
5.88	12th harmonic
7.35	15th harmonic
Higher harmonics appeared to be present but were difficult to distinguish	
30	generator frequency

**Table 2: Fixed-frequency peaks**

Peak Frequency (Hz)	Comments
0.669	
11	broad peak; 5 - 17 Hz

### *Spectra at Varying Distances*

# Horizontal Motion at Increasing Distances

motion in direction of nearest turbine

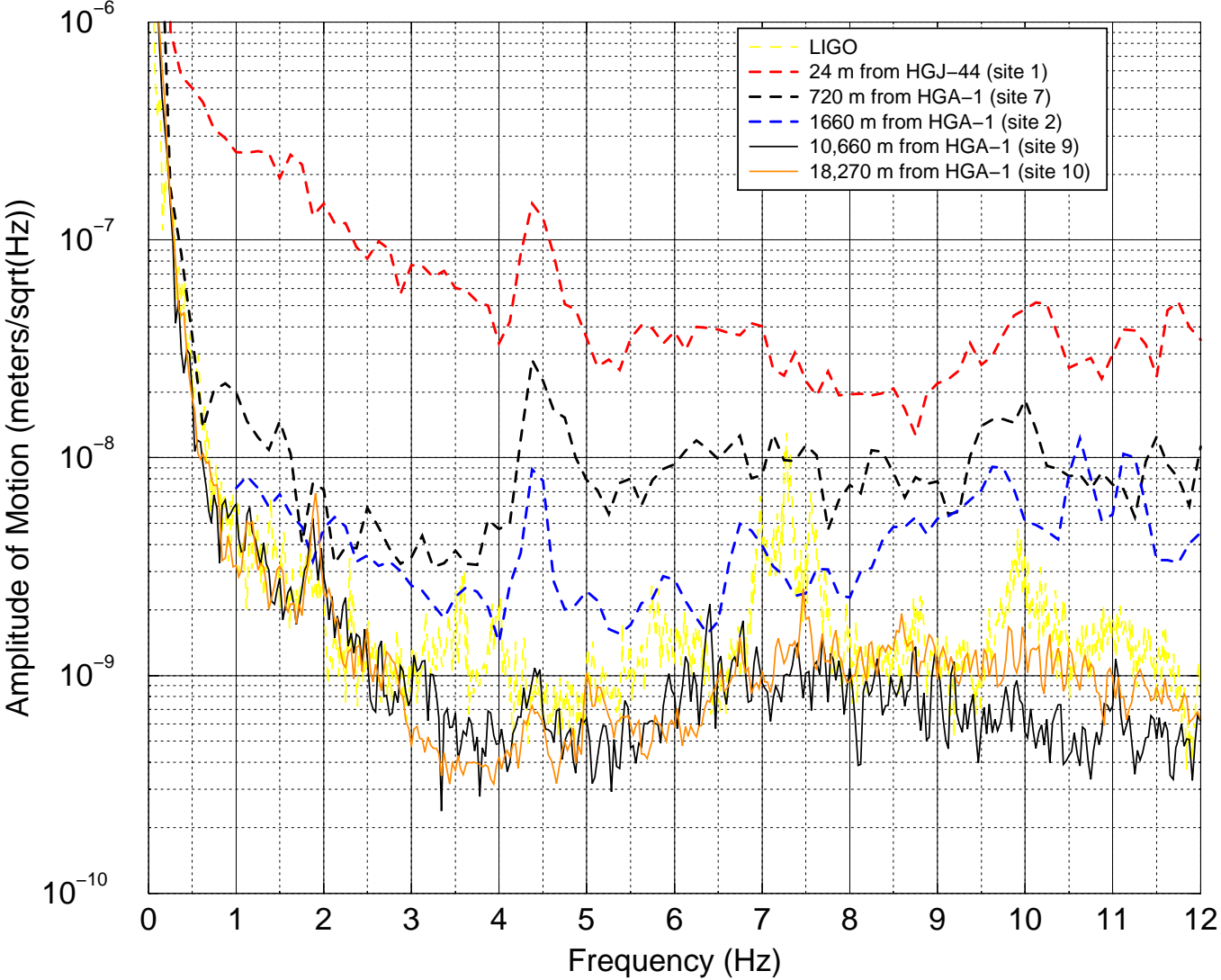


Figure 7.

Figure 7 shows some of the spectra from sites at increasing distances from the Stateline project.

## Analysis

In order to predict signal amplitudes at LIGO, assumptions or models were developed for how signals from multiple turbines at varying distances combine, how the signals propagate, and how the signals vary with different turbine designs and with wind speed.

### Combining Signals from Multiple Turbines in Quadrature

For all calculations here, the signals from multiple turbines were assumed to add in quadrature. Thus, the amplitude of the signal produced by 100 identical turbines at identical distances was assumed to be  $\sqrt{100}$  or 10 times the amplitude of the signal from a single turbine. If the phase angles of each of the 100 turbines were identical and the inter-turbine spacing were small compared to the seismic wavelengths, the signal would be 100 times rather than 10 times the single turbine amplitude. However, in the case of the Stateline project, the phase angles of the turbines were not all identical during power generation - visually the blades were in different positions relative to the tower. This is because the Vestas V-47 generator, while directly connected to the power grid, is an induction generator and so the position of the rotor poles varies relative to the turbine blades. Furthermore, the rotation frequency of the turbines may vary by 10% (OptiSlip) during generation.

### Propagation

Three attenuation models were tested, a  $1/\sqrt{r}$  model with linear attenuation, typical of propagation at the surface of the ground, a  $1/\sqrt{r}$  model (no linear attenuation), and a  $1/r$  model, typical of propagation through the air.

#### *The $1/\sqrt{r}$ with linear attenuation model*

The amplitude of the signal from a single turbine at a distant location,  $A_{far}$ , was assumed to be related to the amplitude at a location closer to the turbine,  $A_{near}$ , by:

$$A_{far} = A_{near} \sqrt{\frac{R_{near}}{R_{far}}} e^{-\frac{\pi f}{Qv}(R_{far} - R_{near})}$$

where  $R_{near}$  and  $R_{far}$  are the distances from the source to the near and far locations, respectively,  $Q$  is a factor giving the non-geometrical attenuation of the wave with distance travelled,  $f$  is the frequency of the signal and  $v$  is its propagation velocity. This formula is applicable to the degree that the waves are surface waves radiating out from the source uniformly (e.g. that there are no reflectors etc.).

Values of  $v \sim 500$  m/s and  $Q \sim 68$  have been measured near LIGO for frequencies of about 5 Hz. For the calculations here,  $Qv$  was assumed to be 34,000 m/s.

***The 1/sqrt(r) model***

This model is a variant of the above model, with no linear attenuation:

$$A_{far} = A_{near} \sqrt{\frac{R_{near}}{R_{far}}}$$

***The 1/r model***

This model is typical of propagation through a volume (as opposed to along a surface), such as air, in which there is minimal linear attenuation:

$$A_{far} = A_{near} \frac{R_{near}}{R_{far}}$$

***Obtaining Distances From the Measurement Sites to Each Individual Turbine***

In order to predict the amplitude of a peak at a certain site using the above models, the distances from each site to each of the hundreds of turbines must be known. To do this, a grid was laid out on a map and the coordinates of turbines and measurement sites were entered into a computer that calculated the distance from each measurement site to each of 399 turbines. To simplify data entry, turbines that were far from measurement sites were clustered into groups and assumed to all be located at a single position. The locations of 31 individual turbines and 29 groups were entered. An uncertainty of 10% or less in the predicted amplitude was estimated by varying the coordinates entered for the groups.

***Normalizing According to Wind Speed***

Since the measurements at various distances were taken at different times and different wind speeds, the measurements were normalized according to wind speed at HGA-1. This is only an approximation because the wind speeds at each turbine are different. The energy in a volume of air goes as the square of its velocity, and the number of volumes that pass by the turbine per second increases linearly with velocity. Thus the available power goes as the cube of velocity. It is assumed here that the power in the seismic signal is proportional to the wind power available to the turbine and thus that the signal amplitude goes as the wind velocity to the 3/2 power.

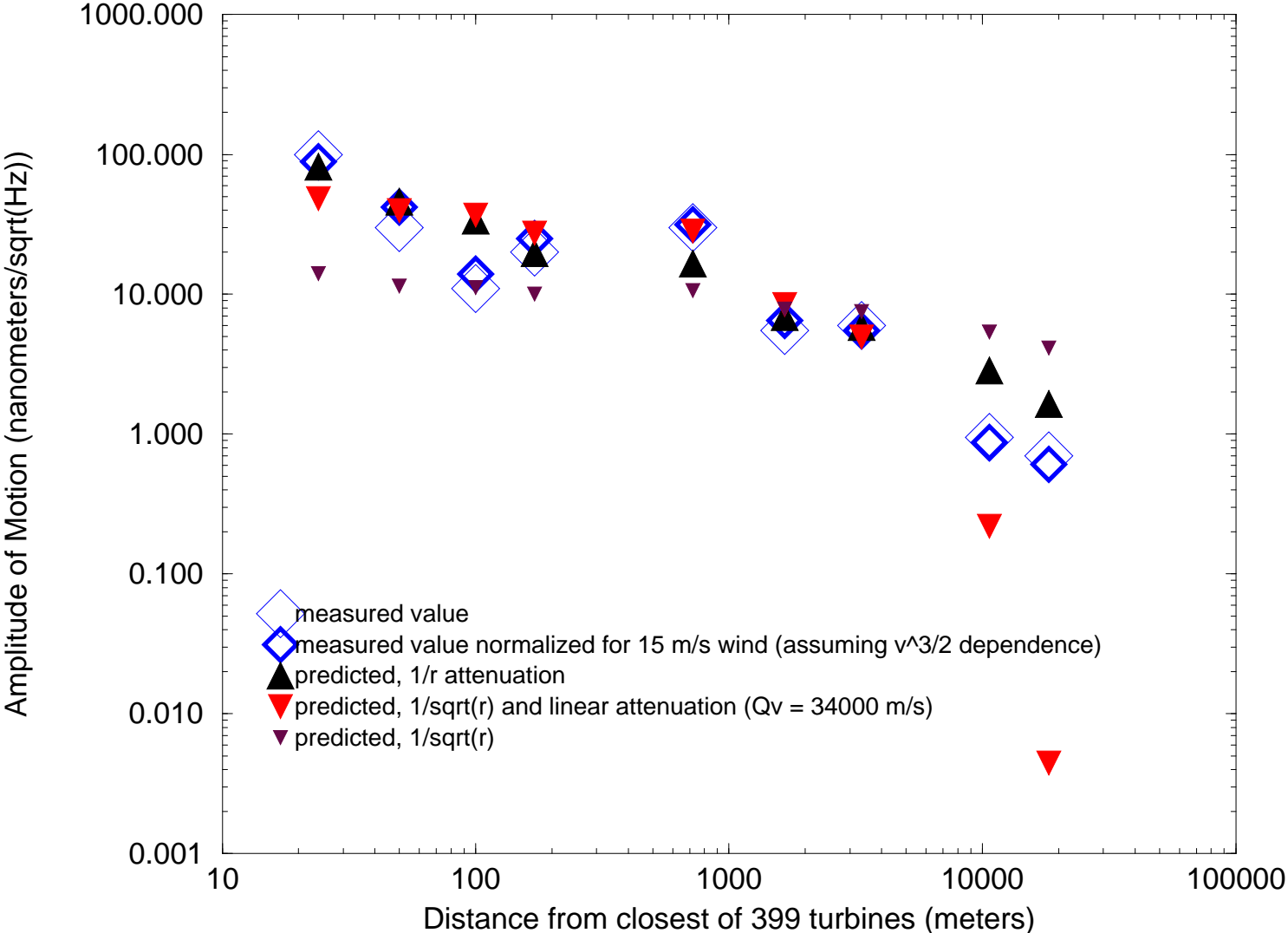
***The 1/r Model Works Best for the 4.34 Hz Peak***

An average value of the peak amplitude of the 4.34 Hz signal was obtained from multiple spectra measured at each site (some of these spectra are shown in Figure 7). These average measured values are shown in Figure 8 as blue diamonds. The 3 propagation models were used to predict the signal from each turbine, assuming that each turbine produced an identical signal. These predicted contributions from the individual turbines were added in quadrature. Rather than obtain  $A_{near}$  in

Figure 8.

### Amplitude of the 4.3 Hz Peak at Various Sites

Note: measurements and predictions contain contributions from 399 turbines up to 11 km apart



the above equations from measurements near the base of one of the turbines, where near-field effects might influence results, the predicted values were normalized as a set to the measured data. This was done “by eye”, adjusting each set of predicted values with a multiplicative constant until about half of the predicted values were above the measured values and about half were below the measured values (see Figure 8). It is clear from Figure 8 that the  $1/r$  model is the most successful in predicting the signal amplitude over long distances. This may indicate that the signal travels partly through the air and couples locally to the ground. A coupling to the ground of a low frequency acoustic signal produced by the turbine blades would be similar to the mechanism by which helicopters shake the ground (at about 10 Hz) when in flight. One test of this hypothesis would be to determine if the propagation velocity of the Stateline signals is that of sound in air. Of course energy from the air signal would be lost to the ground so the signal would attenuate at a rate greater than  $1/r$ . This may partly explain why the two values at the greatest distance fall below the model.

#### ***Evidence that Infra-sound Did Not Couple Directly to the Seismometer***

The possibility that the 4.3 Hz signal was coupling directly to the seismometer was considered. Acoustic coupling at 5 Hz was measured in the laboratory. A microphone and a seismometer were placed near a seismically isolated speaker generating a 5 Hz signal. At Stateline, microphone signals were recorded at several sites along with seismometer signals. The ratio of microphone to seismometer signals at Stateline was much lower than in the acoustic coupling measurement. This indicates that acoustic coupling directly to the seismometer could not account for the seismic signals measured at Stateline.

#### **Differences Between the Stateline Turbines and the Proposed Maiden Turbines**

The turbines for the Maiden site may differ from the Vestas V47 turbines at the Stateline site. A likely candidate for the Maiden site is the GE 1.5MW Turbine. For signal amplitude estimates, it will be assumed that the amplitude of the seismic signal increases as the square root of the turbine power output. Thus the signal produced by a 1.5 MW turbine will be assumed to be 1.51 times greater than that produced by the 660 kW Stateline turbines.

The GE turbine being considered features an indirect grid connection (AC-DC-AC conversion) and generates at rotation frequencies of 0.18 - 0.33 Hz, in contrast with the 0.47 +/- 5% rate of the V47. A possible advantage of variable rate turbines is that the rotation rates of the different turbines at the Maiden site may, at any given time, vary more than the rates of the different turbines at Stateline, producing broader, lower amplitude peaks.

#### **Prediction of the Signal Level at LIGO Produced by the Maiden Wind Project**

This prediction was for the 4.3 Hz peak, which was the largest peak attributed to the turbines that was evident at sites further than 1 km from the nearest turbine. The prediction was based on the measured value at the most distant site from Stateline, an assumption of  $1/r$  propagation, and assumptions about scaling for wind speed and for turbine numbers and power. From the data obtained at site 10 and the distances to each turbine, it was estimated that a single Stateline turbine would produce a 0.038 nanometer per  $\sqrt{\text{Hz}}$  signal at 18 km when the wind speed was 15

m/s. The signal level (nanometers per sqrt(Hz)) that the Maiden project would produce at LIGO ( $A_{LIGO}$ ) was thus estimated as::

$$A_{LIGO} = A_{1SL} \left( \frac{v}{15} \right)^{1.5} \sqrt{N_M} \sqrt{\frac{P_M}{P_{SL}}} \frac{r_1}{R_{MtoLIGO}}$$

Where  $A_{1SL}$  is the amplitude of the signal from 1 stateline turbine at 18 km (0.038 nm/sqrt(Hz)),  $v$  is the wind speed in m/s (15),  $N_M$  is the number of proposed turbines at Maiden (330),  $P_M$  is the power rating of the turbines at Maiden (1.5 MW),  $P_{SL}$  is the power rating of the turbines at Stateline (0.66 MW),  $r_1$  is the distance to the turbine producing the  $A_{1SL}$  signal (18 km), and  $R_{MtoLIGO}$  is the distance from the Maiden site to LIGO (all Maiden turbines were assumed to be at a distance of 20 km). The estimate produced in this manner was 0.94 nm/sqrt(Hz), close to the current LIGO level (about 0.8 nm/sqrt(Hz)) at this frequency.

### ***The high degree of uncertainty***

The uncertainty is primarily due to differences in turbines and to geographic differences between sites.

#### Possible differences in the frequency and magnitude of the predominant peak.

Since the proposed Maiden turbines will be larger and operate at a lower frequency, the frequencies of the peaks will differ from the Stateline frequencies. It is not clear why the 9th harmonic of the Stateline turbine rotation rate is the predominant peak. If it is because the 4.3 Hz peak is in a band that couples well to the ground, the frequency of the peak from the Maiden turbines may be close to that of the Stateline turbines, though the 12th or 15th harmonic rather than the 9th harmonic may be emphasized. On the other hand, if the emphasis of the 9th harmonic is related to the width of the blades relative to the distance between blades, the predominant peak from the Maiden turbines may be at a lower frequency than the predominant Stateline frequency. The uncertainty in the signal amplitude due to different rotation rates was estimated to be a factor of two.

#### Differences in rotation rate variation.

The variable rate of the proposed turbines could result in a lower signal level at LIGO, but not in a higher level. If the frequency variation of the Maiden turbines turns out to be about 4 times that of the Stateline turbines, the peak signal would be expected to be reduced by about a factor of 2 from the estimated value.

#### Unknown differences in the turbines and inaccurate assumptions.

These uncertainties were estimated to be about a factor of 2. One possibility is that the signal amplitude does not scale as the square root of the generation power.

#### Uncertainties due to topography.

The topographic relationship of the Maiden site to the LIGO site is similar to the relationship between the Stateline and distant measurement sites. The three measurement sites most distant

from Stateline were off of the basalt ridge on the alluvial plane. LIGO is similarly situated relative to the Maiden site. One difference between the Maiden and Stateline sites is that the basalt is closer to the surface at the Maiden site than at the Stateline site. It seems unlikely that topographic differences would amount to more than a factor of 2 difference in signal level.

### **Conclusion and Recommendation**

In summary, it is likely that the largest peak produced by the Maiden project would be larger than 1/7 of the LIGO background and smaller than 7 times the LIGO background when the wind speed at the Maiden site was about 15 m/s (about 34 mph). At higher wind speeds the signal would be larger, though the background level would increase with increasing wind speed at LIGO.

Seismic measurements at a site employing the turbines that will be used for the Maiden project could significantly reduce this uncertainty and are recommended.

# **Seismic Measurements at the Stateline Wind Project**

## **And A Prediction of the Seismic Signal that the Proposed Maiden Wind Project Would Produce at LIGO**

**Robert Schofield, Ph.D., University of Oregon**

### **Summary**

**Measurements of ground vibration were made at 10 sites around the Stateline Wind Project. The 3-bladed turbines produce seismic peaks mainly at multiples of 3 times their rotation frequency. The strongest peak (4.3 Hz) was detected at a site about 18 km from Stateline where it reached 0.7 nm/sqrt(Hz) of ground motion. Signal amplitudes were fit best with a  $1/r$  attenuation model, suggesting that the propagation path is partly through the air. The signal level that the Maiden project (both phases) would produce at the LIGO site (about 20 km distant) was estimated, with a high degree of uncertainty, to be about equal to the present background level at LIGO.**

**The accuracy of the predictions could be improved by measurements at a site that uses the turbines planned for the Maiden project. For example, it is possible that the rotation rate of the Maiden turbines would vary to a degree that the peaks from the individual turbines did not “pile up” as much at a particular frequency. Measurements at a site that employs the proposed Maiden turbines are recommended.**

### **Motivation**

The Laser Interferometric Gravitational wave Observatory (LIGO) on the Hanford reservation is concerned that the seismic signal from the Maiden wind project may shake precisely positioned mirrors. Perhaps the greatest danger to LIGO is that one (or more) of the potential peaks from the Maiden site match the frequency of a resonance in the seismic isolation system. An example of such an unlucky coincidence is a 2.3 Hz peak (from cooling tower fans at a nearby nuclear power plant) that exceeds the surrounding background at LIGO by only a factor of about 5. Because it matches a seismic isolation system resonance, this peak is responsible for about 20% of the r.m.s. of the frequency noise in one interferometer, prior to special servo modification. A similar amplitude signal from the Maiden Wind Project, at a resonance, could contribute much more to this r.m.s. because the peak would be wider. This could create a need for abatement modifications.

### **Measurements**

#### **Instrumentation**

Seismic measurements were made using a Guralp CMG-40T seismometer whose outputs were fed through a Stanford SR-560 preamplifier into an HP 3857 signal analyzer. Instruments were powered by internal or external (automobile) batteries. At sites 1 and 2, the seismometer was placed on a granite slab set directly on the earth at the bottom of a meter deep pit (Figure 1). The pit was walled and capped with a wooden box. The box top was then covered with a couple of inches of earth to bring the level up to the surrounding grade. At other sites, the seismometer was shielded from wind using an overturned plastic tub instead of a pit.



**Figure 1.** Seismometer in pit at site 2.

## Calibration

The instrumentation described above was set up, using identical instrument settings, near a LIGO seismometer. The signal level calculated from the HP 3857 output, using the manufacturer's calibration, matched the signal level output by the LIGO data system. Noise floors for each of the instrument settings used during data collection at the Stateline site were determined by replacing the seismometer with a resistor matched to the seismometer output resistance. Noise floors were below signal level for spectra shown here.

## Results

### *Measurement Locations*

Measurements were made at 10 locations. Seismometer pits were excavated at two sites. Site 1 was located 24 meters SW of the base of turbine HGJ-44 (Figure 2). Site 2 was located 1660 m (about 1 mile) from HGA-1 and is shown on the map of Figure 3. At the other locations, plastic tubs were used instead of pits. These locations were as follows: site 3, on the cement base of HGJ-44, site 4, 50 meters from HGA-1 (Fig. 3), site 5, 100 meters from HGA-1 on Hatch Grade Rd. (Fig. 3), site 6, 150 m from the base of HGA-1 at the corner of Hatch Grade and Braden Ranch roads (Fig. 3), site 7, located 710 m from HGA-1 on Hatch Grade road (Fig. 3), site 8, about 3 km from HGA-1, across the Walla Walla river (Fig. 4), site 9, about 11 km away on Dodd road (Fig. 4), and, site 10, about 18 km away in



**Figure 2.** Site 1: the pit was in the shadow of the mound at the lower left; the base of HGJ-44 is 24 m away in the near background

the McNary National Wildlife Refuge (Fig. 4).

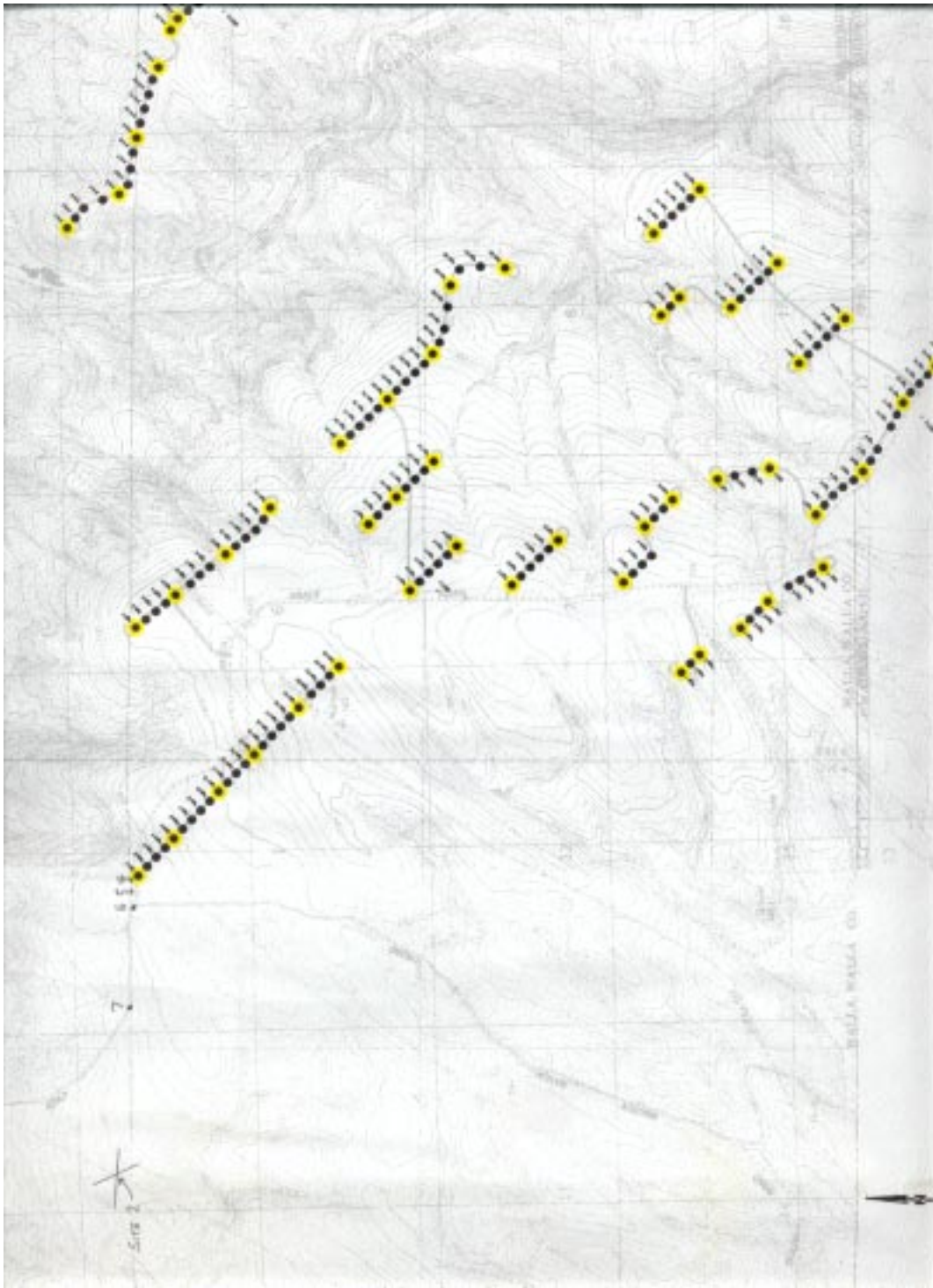


Figure 3



**Figure 4.**

### *Spectra*

Figures 5 and 6 show spectra from sites 1 and 2. The figures show a low frequency and a high frequency measurement for each site. The LIGO spectra were taken the same evening as the Maiden spectra; the wind speed at LIGO for this data averaged about 8 m/s.

Figure 5.

### Vertical Motion at Sites 1 & 2

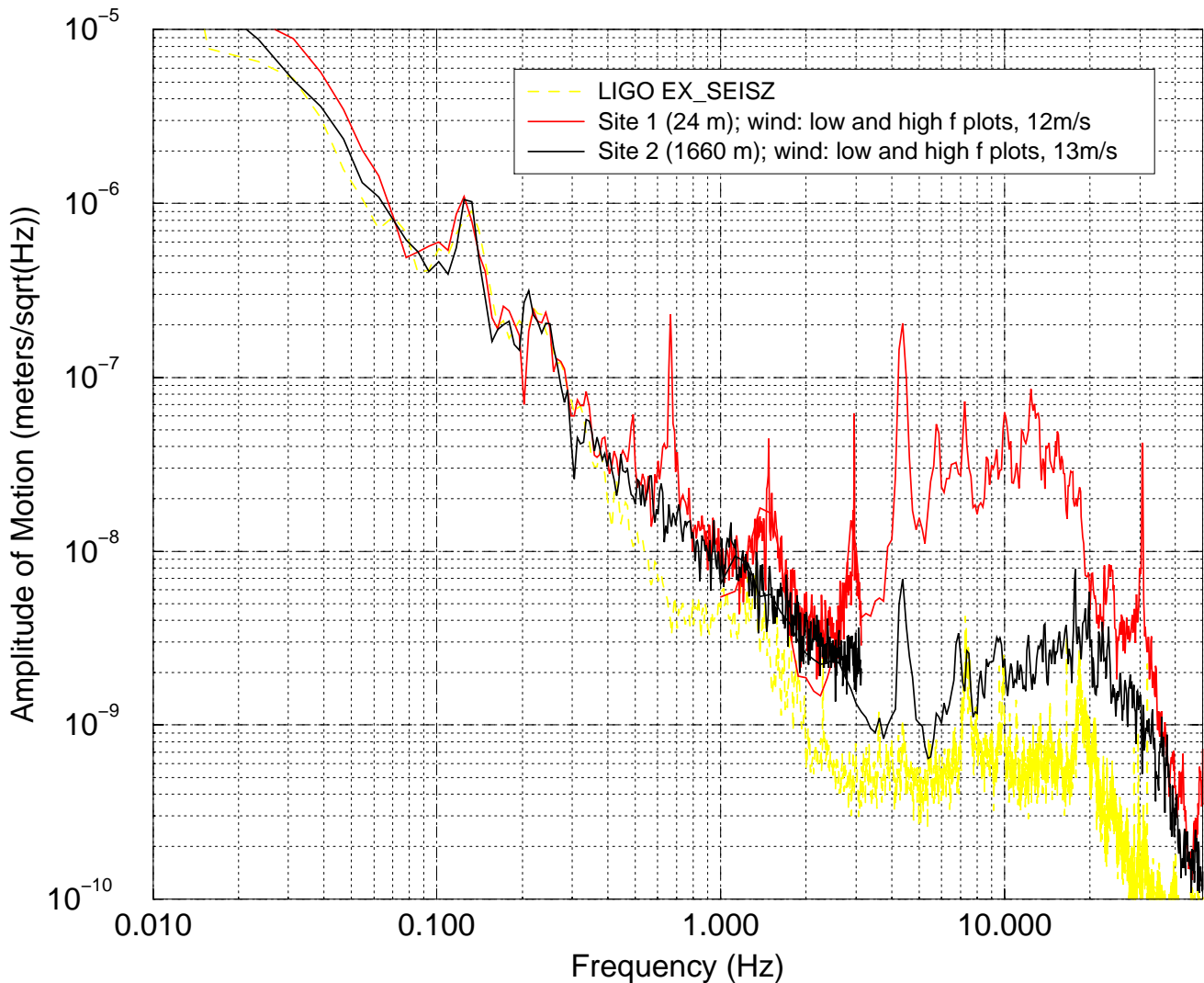
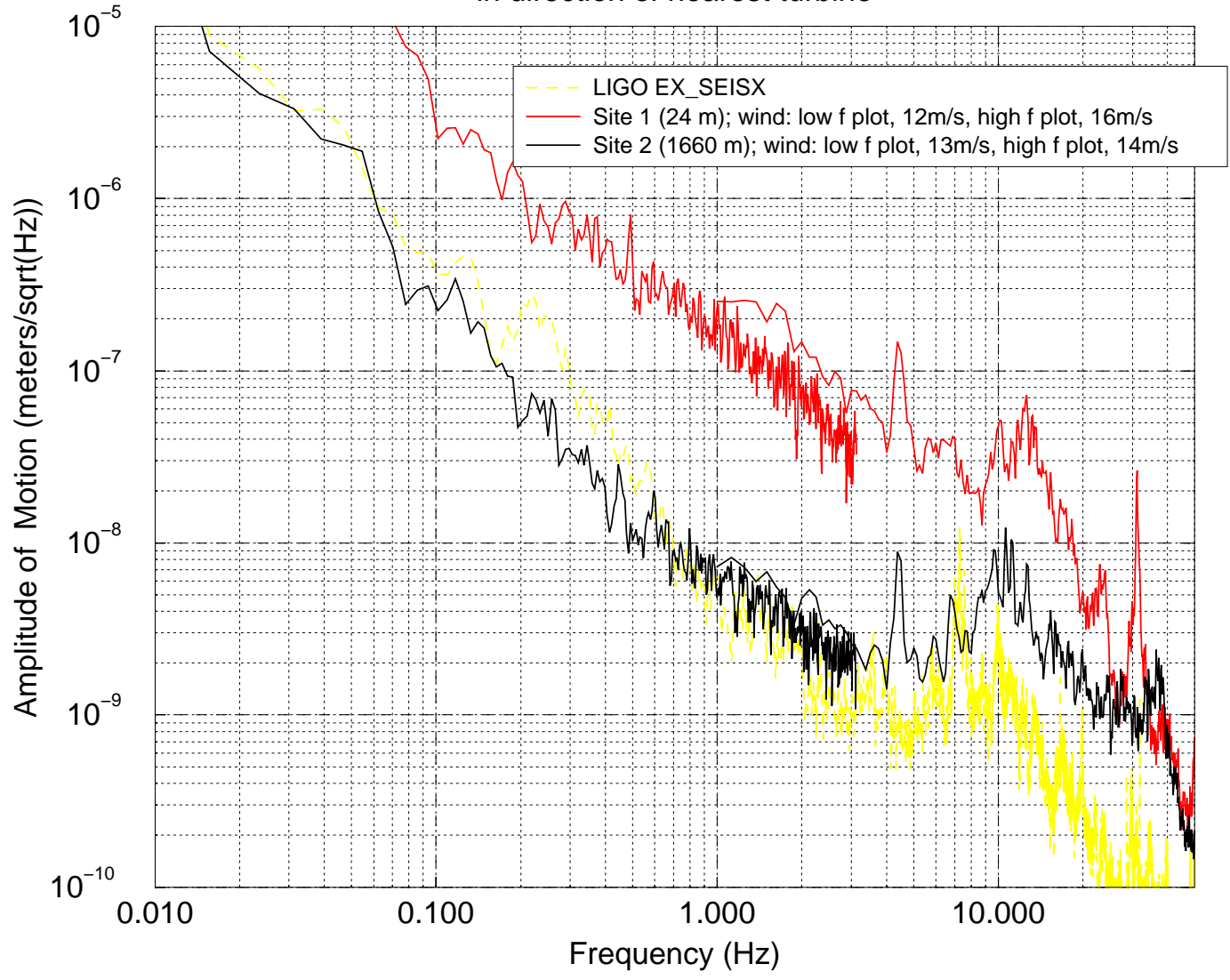


Figure 6.

# Horizontal Motion at Sites 1 & 2

in direction of nearest turbine



### *Signal Identification*

Signals were attributed to the turbines if they were relatively larger nearer to the base of the tower. Two types of peaks were identified, stationary frequency peaks, presumably associated with structural resonances, and peaks whose frequency varied with turbine rotation rate. To discriminate between these two types, a seismometer was set up on the base of a turbine tower (site 3) during a period of low wind velocity, when many turbines were not moving. The peaks identified below as stationary were observed at the same frequency as during high wind velocity periods. The peaks identified as varying were observed to increase in frequency as the rotation rate of the turbine increased. At higher wind velocities these varying frequencies stabilize because the turbine is designed to run at a nearly constant rotation rate (OptiSlip-equipped induction generators allow about a 10% variation in rate).

**Table 1: Peaks that decreased in frequency at low wind velocities**

Approximate frequency at high wind velocity (Hz)	Comments
0.49	rotation frequency of turbine (29 rpm)
1.47	3rd harmonic of rotation frequency (blade pass frequency)
2.95	6th harmonic
4.34	9th harmonic (largest peak relative to background)
5.88	12th harmonic
7.35	15th harmonic
Higher harmonics appeared to be present but were difficult to distinguish	
30	generator frequency

**Table 2: Fixed-frequency peaks**

Peak Frequency (Hz)	Comments
0.669	
11	broad peak; 5 - 17 Hz

### *Spectra at Varying Distances*

Figure 7.

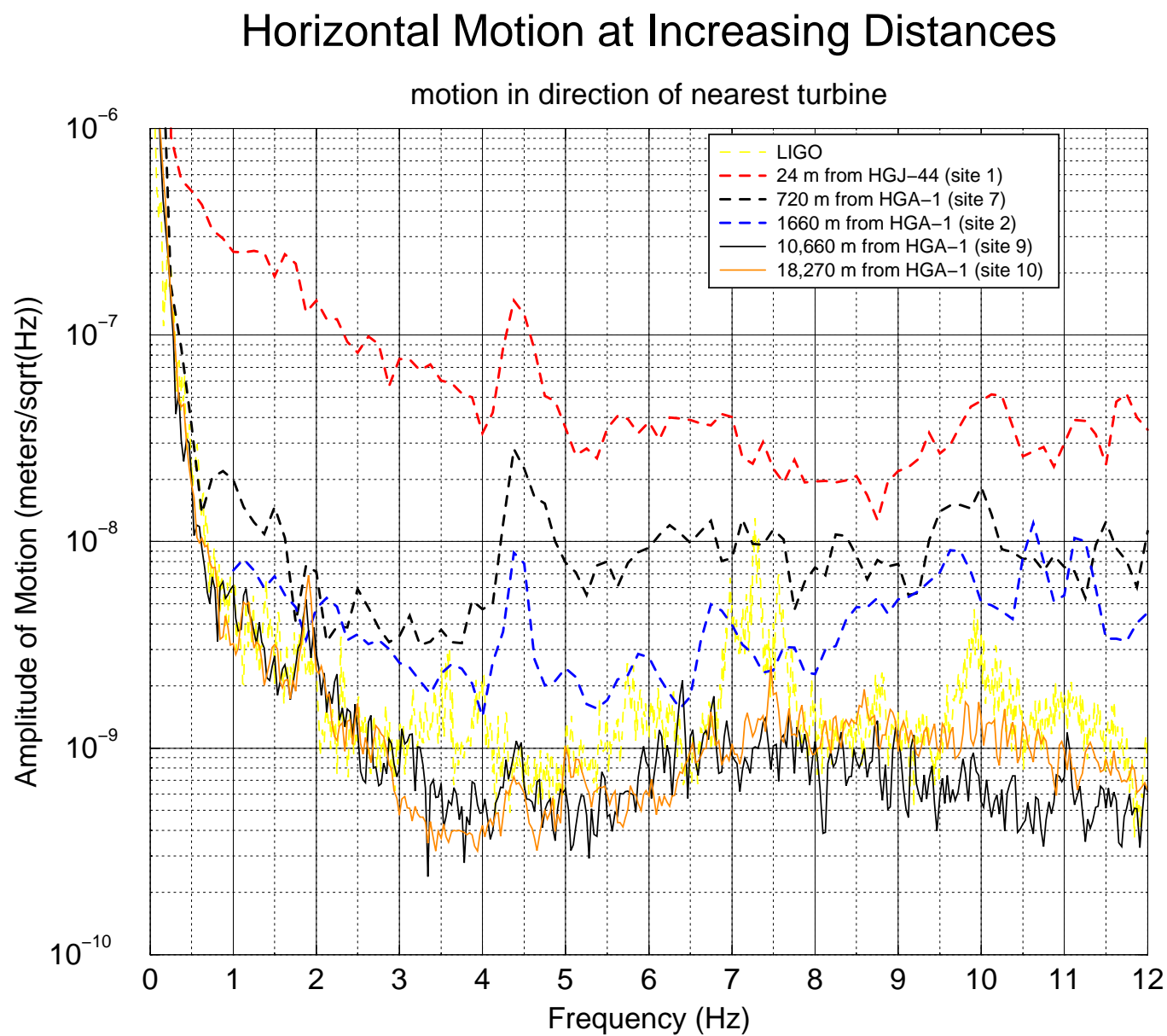


Figure 7 shows some of the spectra from sites at increasing distances from the Staveland project.

## Analysis

In order to predict signal amplitudes at LIGO, assumptions or models were developed for how signals from multiple turbines at varying distances combine, how the signals propagate, and how the signals vary with different turbine designs and with wind speed.

### Combining Signals from Multiple Turbines in Quadrature

For all calculations here, the signals from multiple turbines were assumed to add in quadrature. Thus, the amplitude of the signal produced by 100 identical turbines at identical distances was assumed to be  $\sqrt{100}$  or 10 times the amplitude of the signal from a single turbine. If the phase angles of each of the 100 turbines were identical and the inter-turbine spacing were small compared to the seismic wavelengths, the signal would be 100 times rather than 10 times the single turbine amplitude. However, in the case of the Stateline project, the phase angles of the turbines were not all identical during power generation - visually the blades were in different positions relative to the tower. This is because the Vestas V-47 generator, while directly connected to the power grid, is an induction generator and so the position of the rotor poles varies relative to the turbine blades. Furthermore, the rotation frequency of the turbines may vary by 10% (OptiSlip) during generation.

### Propagation

Three attenuation models were tested, a  $1/\sqrt{r}$  model with linear attenuation, typical of propagation at the surface of the ground, a  $1/\sqrt{r}$  model (no linear attenuation), and a  $1/r$  model, typical of propagation through the air.

#### *The $1/\sqrt{r}$ with linear attenuation model*

The amplitude of the signal from a single turbine at a distant location,  $A_{far}$ , was assumed to be related to the amplitude at a location closer to the turbine,  $A_{near}$ , by:

$$A_{far} = A_{near} \sqrt{\frac{R_{near}}{R_{far}}} e^{-\frac{\pi f}{Qv}(R_{far} - R_{near})}$$

where  $R_{near}$  and  $R_{far}$  are the distances from the source to the near and far locations, respectively,  $Q$  is a factor giving the non-geometrical attenuation of the wave with distance travelled,  $f$  is the frequency of the signal and  $v$  is its propagation velocity. This formula is applicable to the degree that the waves are surface waves radiating out from the source uniformly (e.g. that there are no reflectors etc.).

Values of  $v \sim 500$  m/s and  $Q \sim 68$  have been measured near LIGO for frequencies of about 5 Hz. For the calculations here,  $Qv$  was assumed to be 34,000 m/s.

***The 1/sqrt(r) model***

This model is a variant of the above model, with no linear attenuation:

$$A_{far} = A_{near} \sqrt{\frac{R_{near}}{R_{far}}}$$

***The 1/r model***

This model is typical of propagation through a volume (as opposed to along a surface), such as air, in which there is minimal linear attenuation:

$$A_{far} = A_{near} \frac{R_{near}}{R_{far}}$$

***Obtaining Distances From the Measurement Sites to Each Individual Turbine***

In order to predict the amplitude of a peak at a certain site using the above models, the distances from each site to each of the hundreds of turbines must be known. To do this, a grid was laid out on a map and the coordinates of turbines and measurement sites were entered into a computer that calculated the distance from each measurement site to each of 399 turbines. To simplify data entry, turbines that were far from measurement sites were clustered into groups and assumed to all be located at a single position. The locations of 31 individual turbines and 29 groups were entered. An uncertainty of 10% or less in the predicted amplitude was estimated by varying the coordinates entered for the groups.

***Normalizing According to Wind Speed***

Since the measurements at various distances were taken at different times and different wind speeds, the measurements were normalized according to wind speed at HGA-1. This is only an approximation because the wind speeds at each turbine are different. The energy in a volume of air goes as the square of its velocity, and the number of volumes that pass by the turbine per second increases linearly with velocity. Thus the available power goes as the cube of velocity. It is assumed here that the power in the seismic signal is proportional to the wind power available to the turbine and thus that the signal amplitude goes as the wind velocity to the 3/2 power.

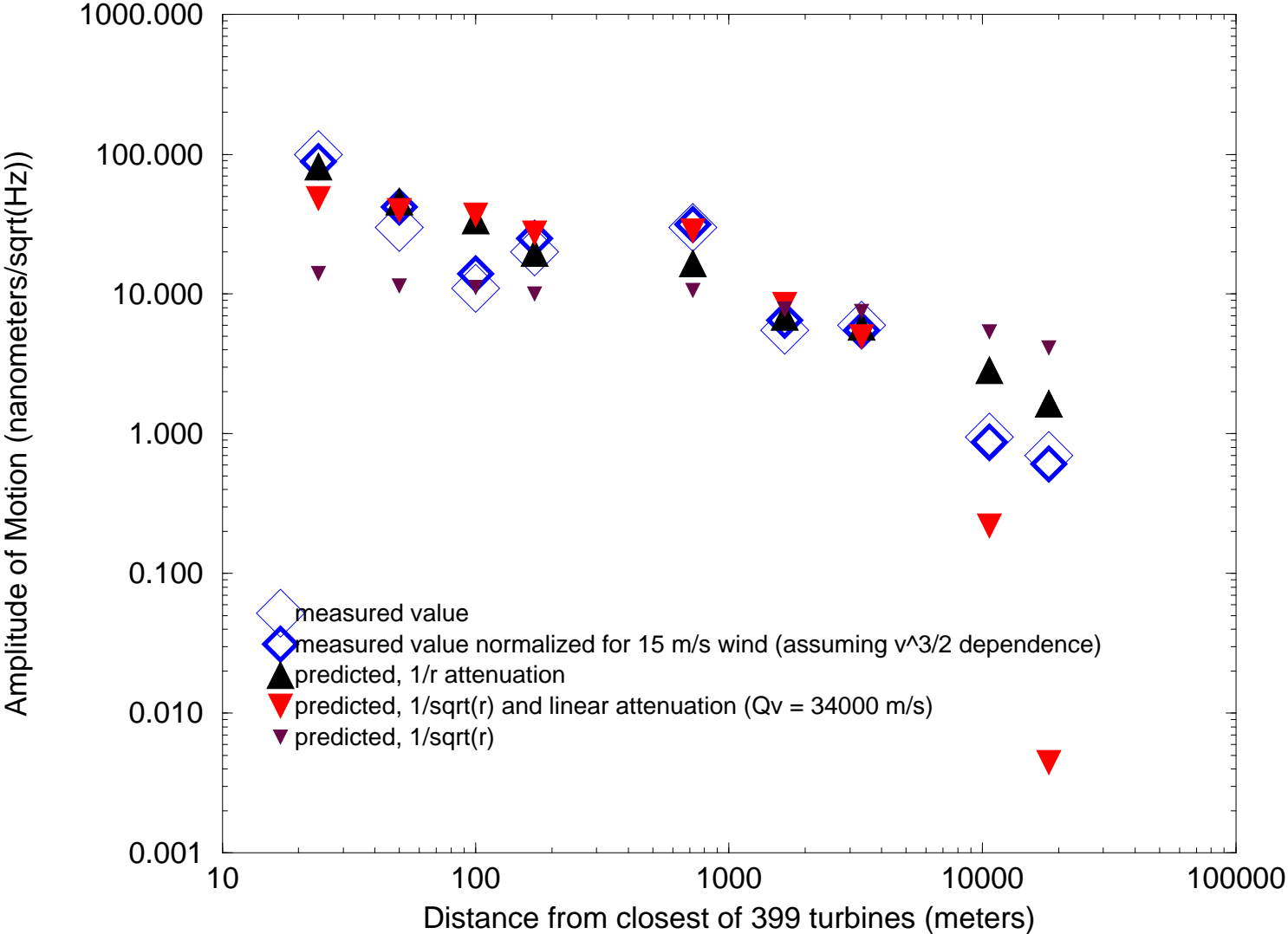
***The 1/r Model Works Best for the 4.34 Hz Peak***

An average value of the peak amplitude of the 4.34 Hz signal was obtained from multiple spectra measured at each site (some of these spectra are shown in Figure 7). These average measured values are shown in Figure 8 as blue diamonds. The 3 propagation models were used to predict the signal from each turbine, assuming that each turbine produced an identical signal. These predicted contributions from the individual turbines were added in quadrature. Rather than obtain  $A_{near}$  in

Figure 8.

### Amplitude of the 4.3 Hz Peak at Various Sites

Note: measurements and predictions contain contributions from 399 turbines up to 11 km apart



the above equations from measurements near the base of one of the turbines, where near-field effects might influence results, the predicted values were normalized as a set to the measured data. This was done “by eye”, adjusting each set of predicted values with a multiplicative constant until about half of the predicted values were above the measured values and about half were below the measured values (see Figure 8). It is clear from Figure 8 that the  $1/r$  model is the most successful in predicting the signal amplitude over long distances. This may indicate that the signal travels partly through the air and couples locally to the ground. A coupling to the ground of a low frequency acoustic signal produced by the turbine blades would be similar to the mechanism by which helicopters shake the ground (at about 10 Hz) when in flight. One test of this hypothesis would be to determine if the propagation velocity of the Stateline signals is that of sound in air. Of course energy from the air signal would be lost to the ground so the signal would attenuate at a rate greater than  $1/r$ . This may partly explain why the two values at the greatest distance fall below the model.

#### ***Evidence that Infra-sound Did Not Couple Directly to the Seismometer***

The possibility that the 4.3 Hz signal was coupling directly to the seismometer was considered. Acoustic coupling at 5 Hz was measured in the laboratory. A microphone and a seismometer were placed near a seismically isolated speaker generating a 5 Hz signal. At Stateline, microphone signals were recorded at several sites along with seismometer signals. The ratio of microphone to seismometer signals at Stateline was much lower than in the acoustic coupling measurement. This indicates that acoustic coupling directly to the seismometer could not account for the seismic signals measured at Stateline.

#### **Differences Between the Stateline Turbines and the Proposed Maiden Turbines**

The turbines for the Maiden site may differ from the Vestas V47 turbines at the Stateline site. A likely candidate for the Maiden site is the GE 1.5MW Turbine. For signal amplitude estimates, it will be assumed that the amplitude of the seismic signal increases as the square root of the turbine power output. Thus the signal produced by a 1.5 MW turbine will be assumed to be 1.51 times greater than that produced by the 660 kW Stateline turbines.

The GE turbine being considered features an indirect grid connection (AC-DC-AC conversion) and generates at rotation frequencies of 0.18 - 0.33 Hz, in contrast with the 0.47 +/- 5% rate of the V47. A possible advantage of variable rate turbines is that the rotation rates of the different turbines at the Maiden site may, at any given time, vary more than the rates of the different turbines at Stateline, producing broader, lower amplitude peaks.

#### **Prediction of the Signal Level at LIGO Produced by the Maiden Wind Project**

This prediction was for the 4.3 Hz peak, which was the largest peak attributed to the turbines that was evident at sites further than 1 km from the nearest turbine. The prediction was based on the measured value at the most distant site from Stateline, an assumption of  $1/r$  propagation, and assumptions about scaling for wind speed and for turbine numbers and power. From the data obtained at site 10 and the distances to each turbine, it was estimated that a single Stateline turbine would produce a 0.038 nanometer per  $\sqrt{\text{Hz}}$  signal at 18 km when the wind speed was 15

m/s. The signal level (nanometers per sqrt(Hz)) that the Maiden project would produce at LIGO ( $A_{LIGO}$ ) was thus estimated as::

$$A_{LIGO} = A_{1SL} \left( \frac{v}{15} \right)^{1.5} \sqrt{N_M} \sqrt{\frac{P_M}{P_{SL}}} \frac{r_1}{R_{MtoLIGO}}$$

Where  $A_{1SL}$  is the amplitude of the signal from 1 stateline turbine at 18 km (0.038 nm/sqrt(Hz)),  $v$  is the wind speed in m/s (15),  $N_M$  is the number of proposed turbines at Maiden (330),  $P_M$  is the power rating of the turbines at Maiden (1.5 MW),  $P_{SL}$  is the power rating of the turbines at Stateline (0.66 MW),  $r_1$  is the distance to the turbine producing the  $A_{1SL}$  signal (18 km), and  $R_{MtoLIGO}$  is the distance from the Maiden site to LIGO (all Maiden turbines were assumed to be at a distance of 20 km). The estimate produced in this manner was 0.94 nm/sqrt(Hz), close to the current LIGO level (about 0.8 nm/sqrt(Hz)) at this frequency.

### ***The high degree of uncertainty***

The uncertainty is primarily due to differences in turbines and to geographic differences between sites.

#### Possible differences in the frequency and magnitude of the predominant peak.

Since the proposed Maiden turbines will be larger and operate at a lower frequency, the frequencies of the peaks will differ from the Stateline frequencies. It is not clear why the 9th harmonic of the Stateline turbine rotation rate is the predominant peak. If it is because the 4.3 Hz peak is in a band that couples well to the ground, the frequency of the peak from the Maiden turbines may be close to that of the Stateline turbines, though the 12th or 15th harmonic rather than the 9th harmonic may be emphasized. On the other hand, if the emphasis of the 9th harmonic is related to the width of the blades relative to the distance between blades, the predominant peak from the Maiden turbines may be at a lower frequency than the predominant Stateline frequency. The uncertainty in the signal amplitude due to different rotation rates was estimated to be a factor of two.

#### Differences in rotation rate variation.

The variable rate of the proposed turbines could result in a lower signal level at LIGO, but not in a higher level. If the frequency variation of the Maiden turbines turns out to be about 4 times that of the Stateline turbines, the peak signal would be expected to be reduced by about a factor of 2 from the estimated value.

#### Unknown differences in the turbines and inaccurate assumptions.

These uncertainties were estimated to be about a factor of 2. One possibility is that the signal amplitude does not scale as the square root of the generation power.

#### Uncertainties due to topography.

The topographic relationship of the Maiden site to the LIGO site is similar to the relationship between the Stateline and distant measurement sites. The three measurement sites most distant

from Stateline were off of the basalt ridge on the alluvial plane. LIGO is similarly situated relative to the Maiden site. One difference between the Maiden and Stateline sites is that the basalt is closer to the surface at the Maiden site than at the Stateline site. It seems unlikely that topographic differences would amount to more than a factor of 2 difference in signal level.

### **Conclusion and Recommendation**

In summary, it is likely that the largest peak produced by the Maiden project would be larger than 1/7 of the LIGO background and smaller than 7 times the LIGO background when the wind speed at the Maiden site was about 15 m/s (about 34 mph). At higher wind speeds the signal would be larger, though the background level would increase with increasing wind speed at LIGO.

Seismic measurements at a site employing the turbines that will be used for the Maiden project could significantly reduce this uncertainty and are recommended.

**Third International Meeting  
on  
Wind Turbine Noise  
Aalborg Denmark 17 – 19 June 2009**

**A study of the seismic disturbance produced by the wind park near  
the gravitational wave detector GEO-600**

**Irene Fiori<sup>1</sup>, Lara Giordano<sup>2</sup>, Stephan Hild<sup>3</sup>, Giovanni Losurdo<sup>4</sup>, Emanuele Marchetti<sup>6</sup>, Gillian Mayer<sup>3</sup>, Federico Paoletti<sup>1,5</sup>**

*(1) European Gravitational Observatory, S.Stefano a Macerata, Pisa, Italy;*

*(2) University of Salerno, and INFN sez. Napoli, Italy;*

*(3) Albert Einstein Institut and University of Hannover, Germany;*

*(4) INFN, sez. Firenze, Italy;*

*(5) INFN, sez. Pisa, Italy;*

*(6) University of Firenze, Dept. Of Earth Science, Italy.*

[Irene.Fiori@ego-gw.it](mailto:Irene.Fiori@ego-gw.it), [Federico.Paoletti@ego-gw.it](mailto:Federico.Paoletti@ego-gw.it)

## **Abstract**

Noise emissions from wind turbines might disturb the operation and deteriorate the sensitivity of Gravitational Wave (GW) detectors. These detectors aim to an extremely precise measurement (of the order of  $10^{-18}$ m) of the difference in path lengths between interfering light beams from two optical cavities. Seismic ground vibrations and air pressure waves in the low frequency might couple to the detector especially in correspondence to mechanical modes of the seismic isolation system. A wind turbine park exists in the vicinity of the German GW detector GEO-600 (near Hannover) and two parks are planned for construction close to the detector VIRGO in Italy (near Pisa) which has enhanced sensitivity to low frequency GW signals. We have studied some characteristics of the seismic noise emission of the wind park near GEO-600, and developed a simplified model of the attenuation of the seismic wave. We used the model to predict the excess seismic noise that a wind park might produce near VIRGO, and to set a safety distance from the detector for the location of the new wind parks.

## Introduction

Several detectors are nowadays operative to reveal the space-time deformations which, according to Einstein theory of general relativity, are produced when large massive objects undergo fast acceleration variation. Detectable gravitational waves are expected to be produced in astrophysical processes, like supernova explosions, coalescence of binary systems, spinning neutron stars. A class of GW detectors works on the principle of the Michelson interferometer [1]. A laser beam is split in two by a semi-reflective mirror. The two beams are made to resonate in two long orthogonal optical cavities (arms) consisting of one pair of “free falling” mirrors. A gravitational wave would cause a differential variation of the length of the two arms (one stretches a tiny bit, while the other compresses). This results in a phase difference of the two beams which is measured with a photodiode looking at the interference of the beams out of the two arms. Detectors of this kind are: GEO-600 in Germany, VIRGO in Italy, LIGO detectors in USA, TAMA in Japan [2]. These are able to measure a length variation of the order of  $10^{-18}$ m over a 3km distance, and over a frequency band of 10Hz to 10kHz. Second generation detectors, now in construction phase, aim to measurements at least ten times more accurate.

Optical cavity mirrors and benches (carrying optics used for readout and control) are decoupled from ground through seismic isolation systems. These are typically effective above about 10 Hz. Intense low frequency seismic noise might overcome the isolation system and deteriorate the detector sensitivity. A major concern is that low frequency periodic disturbances might match and excite the low frequency modes of the isolation systems, seriously compromising its operation.

In 2004 the EGO laboratory (hosting the VIRGO detector) was notified that two wind parks were planned for construction in its vicinity (few km away from VIRGO experimental buildings). A concern arose about the possible effects of such plants on the detector operation. In particular, the EGO laboratory was interested to assess which would be the effect of such plants in terms of increase of the local anthropogenic background noise, and of the frequency content of the noise which might match critical resonant modes of VIRGO.

A work by Schofield (2001, [3]) had shown that wind turbines produce intense low frequency seismic disturbances that might be still effective (above the local anthropogenic seismic background) at considerably large distance (10-20 km) from turbines. This is confirmed also by the comprehensive and detailed work by Style (2005, [4]) whose report is successive to the time of our study.

Indeed, the seismic excess as function of distance from the plant does depend on the absorption characteristics of the soil, i.e. its composition (rocks or limes) and on the anthropogenic background noise level. A wind park (“Schliekum”) does exist in the vicinity of the GEO-600 detector. Its effect on the site seismicity and on the detector had not been studied, although no significant effect had been ever noticed. However, the VIRGO has enhanced (ten times better) sensitivity in the low

frequencies (10-100Hz) and a different isolation system design, and the impact of wind turbines noise might be more relevant.

The authors performed a study of the seismic noise emissions of the wind park near GEO-600. The soil composition of the GEO site (cultivated soil, and layers of lime and sand deposits) and its seismicity (industrial area, with high density population and road traffic) are similar to those of the VIRGO site. This fact permits a reasonable extrapolation of the data to the VIRGO case. Measurements were carried out during four days in July 2005. A first report was presented at [5]. The study had two main goals: (i) assess and quantify the presence of a seismic wave field from the wind park at the GEO site, (ii) derive a model of the seismic wave absorption which would permit to reasonably quantify the impact of the planned wind parks near EGO, and eventually to define a distance of respect from EGO for the turbines location.

Here below: Section 1 describes measurement location and equipment; Section 2 describes some characteristics of the wind park seismic emissions; Section 3 describes the study of turbines-induced seismicity at GEO site and measurements of the velocity of the seismic wave field derived from correlation measurements with an array of seismometers working in coincidence; Section 4 describes a measurement and modelling of the attenuation of the seismic wave with distance; Section 5 describes the use of the model to predict the turbine noise impact for VIRGO.

## **1. Measurement sites and equipment**

The GEO-600 site is located 25 km South of the city of Hannover in Germany (Figure 1). The detector is surrounded by agricultural cultivated soils. Soil is composed, up to a depth of 20-50m, by lime and sand sediments. Figure 2 shows the site seismicity compared to Peterson LNM, which indicates it to be a relatively high seismicity site. The EGO laboratory site, hosting the VIRGO detector, is located 10 km from the city of Pisa, Italy. The EGO site characteristics are similar to GEO-600 with respect to all mentioned aspects. The seismicity of EGO site is depicted in Figure 2 as well.

The “Schliekum” wind park consists of 8 turbines placed at a distance of 220m to 370m from each other. Turbines are aligned approximately along the North-South direction, at an average distance of 1.0 and 1.6 km respectively from the GEO-600 North and Central experimental buildings (Figure 3).

Schliekum turbines are of different manufacturer and model and differ to some extent in size and power (Table 1). Common relevant features are: (i) a three-bladed rotor head mounted on a steel tower sitting on a concrete foundation; (ii) an active control on the blades pitch angle assure an optimal and constant power output against wind speed changes in the range from 3 to 25 m/s, outside this range windmills are automatically stopped to avoid damage or reduced efficiency. The blades pitch control changes the rotor speed approximately between 9.5 and 20 rmp; (iii) an active control of the nacelle yaw angle keeps the rotor head aligned to the wind direction; (iv) the power generator (asynchronous type, located in the nacelle) runs at variable speed between 700-1400 rmp [6].



Figure 1. Geographical location of the GEO detector (three house markers at center of figure) and wind parks around it: Schliekum wind park (red crosses) and other seven ones (green flag markers).

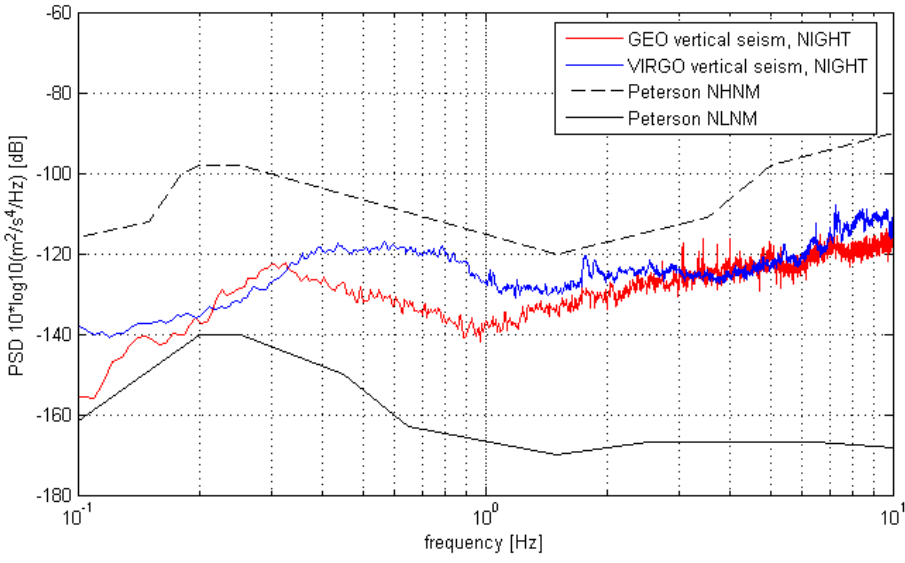


Figure 2. Typical vertical seismic spectra recorded at GEO-600 (red) and VIRGO (blue) experimental buildings during quiet night time periods, compared to Peterson Low and High Noise Models [7].

Manufacturer and Model	N. of turbines	Names	Power [MW]	Tower height [m]	Rotor diameter [m]
Nordex N90	3	Domink, Ole, Malte	2.3	100	90
Nordex S77	2	Daniela, Kerstin	1.5	85	77
EnronWind 1.5s	2	Lutz, Robert	1.5	85	65

EnronWind 1.5	1	Isabelle	1.5	85	65
---------------	---	----------	-----	----	----

Table 1. Tech. data of Schliekum wind turbines. Names have been assigned by us to identify turbines.

A first set of measurements aimed at the characterization of the seismic noise produced by the single turbines. Recordings were taken at the basement platform of each windmill using two geophones (Sercel L-4, 1Hz) laid along the vertical and one horizontal directions. Results are discussed in Section 2.

A second set of measurements aimed at the investigation of the seismic wave-field by the turbines. These data were recorded during July 25<sup>th</sup> through 28<sup>th</sup> 2005. We used: (i) two portable seismic stations, each consisting of one tri-axial low frequency seismometer (Lennartz 3D/5s, 100mHz), AD converter, hard disk, and GPS receiver; and (ii) three fixed tri-axial low frequency seismometers (STS2, 8mHz) permanently deployed on the floor of each GEO-600 experimental building. Seismometers were GPS synchronized, and the 3-axes were aligned along geographical NS, EW and vertical directions ( $\pm 2^\circ$ ). Seismometers were used for coincidence measurements described in Section 3.

We took our own record of the wind speed. We used one anemometer, positioned at 5m height close to GEO-600 central station. However, it is known that wind speed increases logarithmically with height up to some hundreds meters from soil. Therefore, the wind speed values we measured and we quote thorough this report note are systematically lower than wind speed at the turbine blades (80-100m height). Nevertheless, they provide a useful reference for correlation studies (see section 3); but in case we need to compare to wind turbines working set point a scale factor has to be considered.

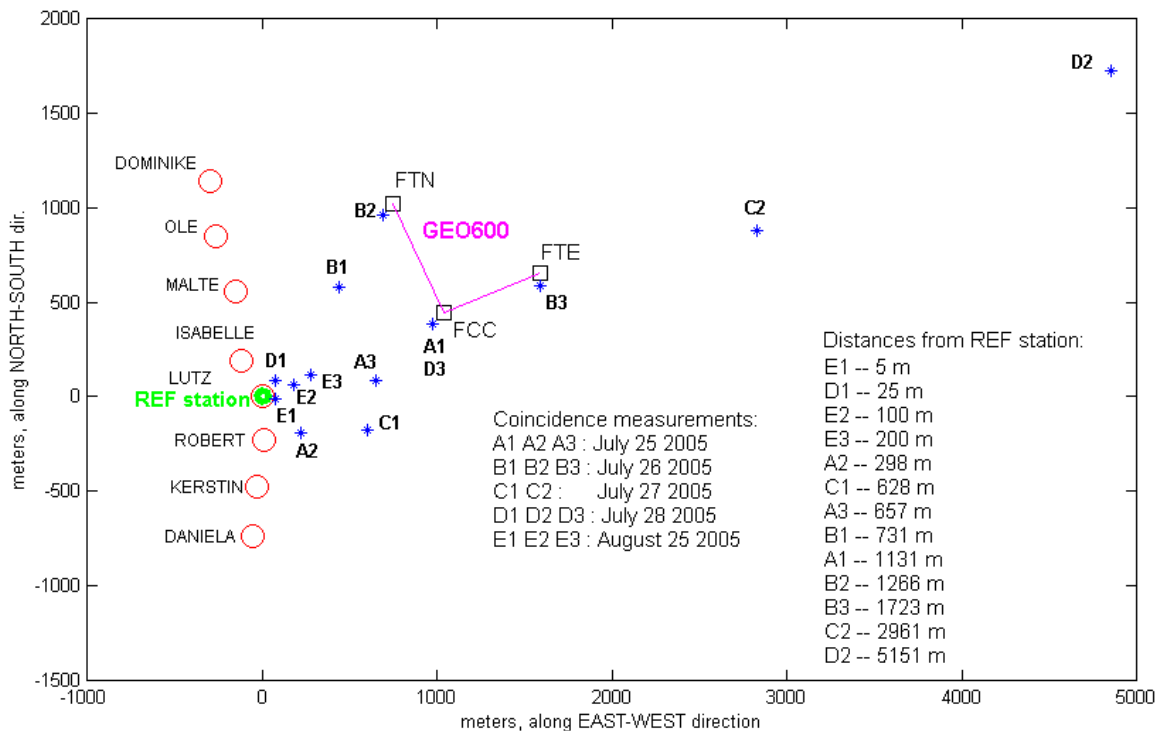


Figure 3. Location of: Schliekum wind turbines (red circles), GEO-600 experimental buildings (black squares), sites of seismic recordings (blue stars), and reference site at turbine “Lutz” (green circle).

## 2. Characteristics of wind turbine seismic emission

Seismic tracks recorded at turbine platforms contain intense and persistent spectral components which can be associated to structural or functional resonances of the windmills. Figure 4 shows the time evolution of the spectral composition of one seismic record. Figure 5 compares spectral composition of seismic records of different turbines. Figure 6 compares the spectral composition of tracks recorded during different wind speed conditions. Figure 7 shows seismic excitations associated to reorientation of one turbine head.

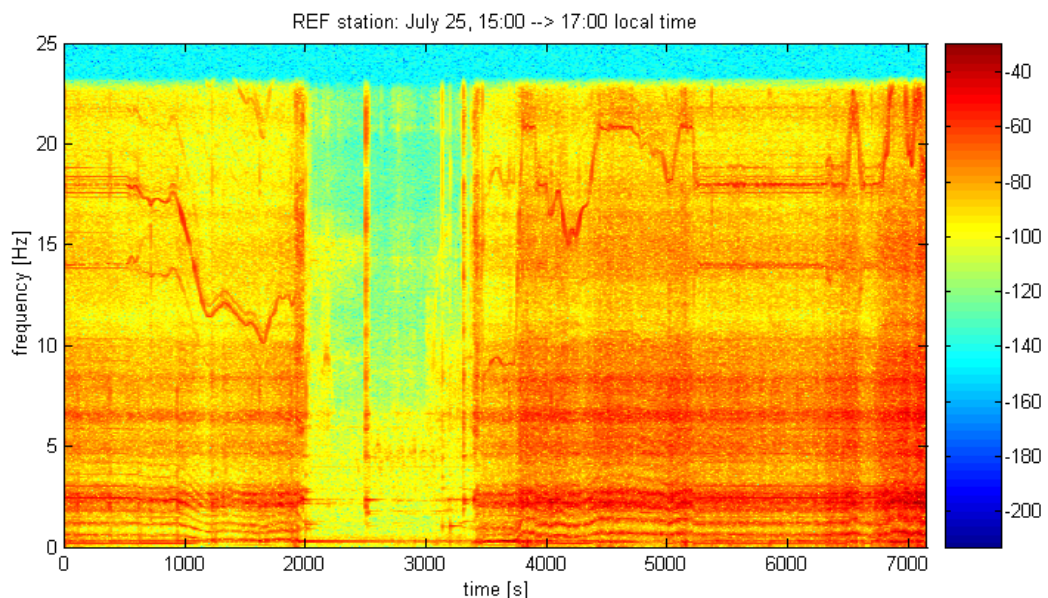
A family of equally spaced and stationary frequency components (we name “functional” peaks) are associated to the revolution frequency of the rotor (around 0.2 Hz) and to the rotor blade-pass frequency (three times the rotor frequency, 0.6 Hz) and its harmonics (1.2Hz, 1.8Hz, 2.4Hz, etc...). Peaks up to the 10<sup>th</sup> harmonic are clearly distinguishable. Often peaks are broad. But sometimes, particularly in conditions of low wind speed, they are very sharp and steady (we suspect that this is associated to a peculiar regime of operation of the turbine feedback control but we do not have records of turbines operation status to investigate further). One intense, always sharp peak sweeping between 10Hz and 20Hz seems associated to the generator frequency (Figure 4, top). All these peaks sometimes do coherent sweeps (frequency changes up to 20%), which look associated to variations of rotor and generator speed (we hypothesize that this occurs when blades pitch angle changes to follow variations of wind speed or direction). Functional peaks disappear when the turbine is stopped (Figure 4).

A few other peaks persist when the turbine is stopped and never change their frequency: the most intense one is around 0.3 Hz (0.37 Hz for the two N77), less intense ones are at 2.5Hz, 4Hz and 6 Hz (Figure 4 and Table 2). These frequencies seem associated to turbine structural modes. According to a simulation study by Shaumann and Seidel [8] the 0.3 Hz frequency might be associated to the pendulum mode of the heavy rotor head and tower, and higher frequencies to flexural modes of the tower.

We took seismic records of the motion of all turbines base platform. We found the amplitude and spectral composition of records of same type turbines are indeed quite similar, while the frequency and shape of peaks differs slightly but significantly among different turbine models (Figure 5).

The root mean square (RMS) of seismic amplitude of the functional peaks increases proportionally to wind speed, and the scaling factor seems the same for all frequencies (Figure 6). Approximately a factor ten variation of RMS is associated to the operation of the turbine at different wind speed conditions within the working range. On the other hand, the amplitude of structural peaks looks independent on wind speed.

Intense seismic bursts with a typical exponential decay (decay time of 1 to 2 minutes) are produced when the turbine head is reoriented in correspondence of wind direction variations. A spectral analysis of the burst signals show that the structural modes are largely excited (2 to 5 times more than during typical conditions). Also some other frequencies (1Hz, 3Hz, and a few above) are excited, which might correspond to other structural modes not much excited during the normal turbine operation.



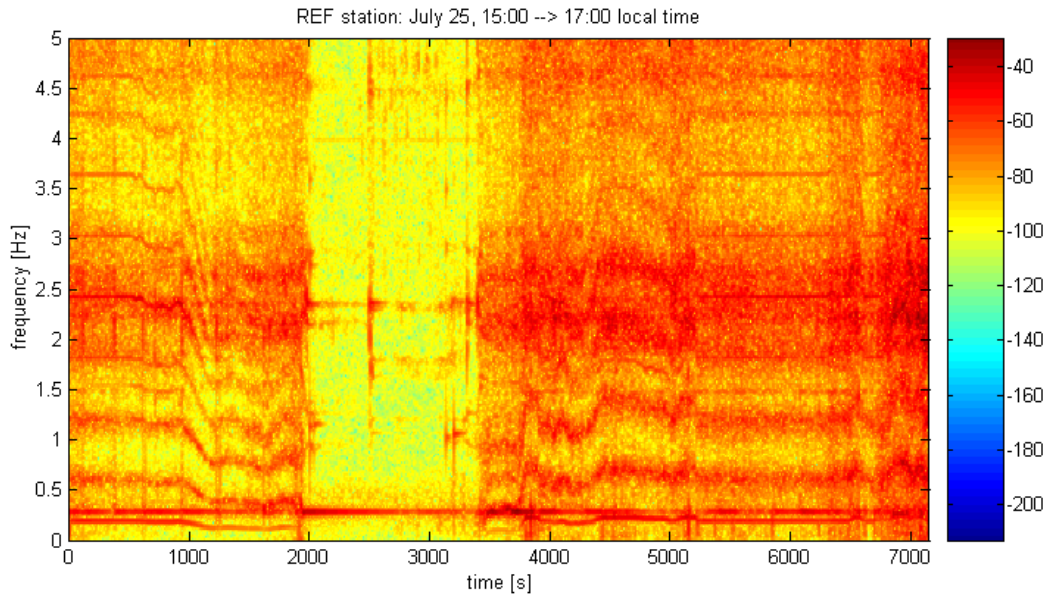
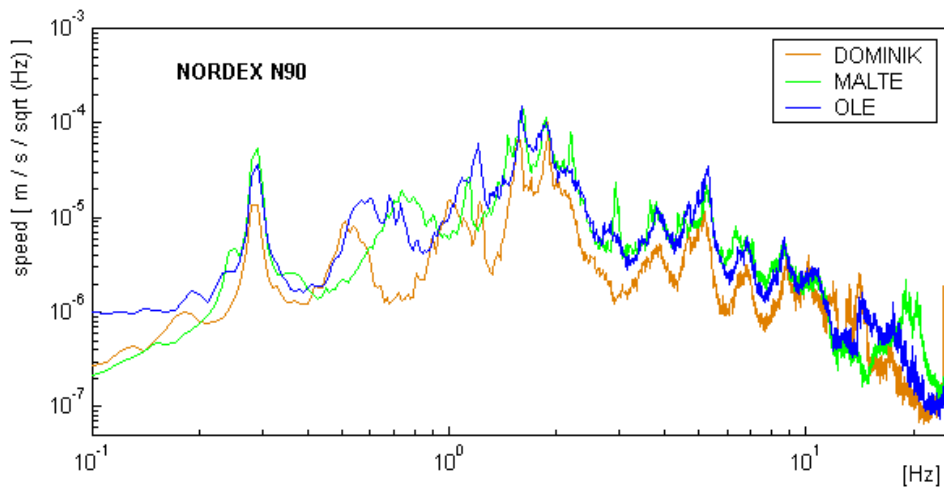


Figure 4. Spectrograms of 2hour seismic record at the Lutz base platform. In the period 2000÷3500s the turbine was stopped. The bottom plot is a zoom of the upper one in the 0÷5 Hz frequency region.

Turbine	Pendulum mode $f_0$ [Hz]	Flexural mode $f_1$ [Hz]
Nordex S77	0.37	2.45
Nordex N90	0.29	1.9
Enron Wind 1.5	0.29	2.3
Enron Wind 1.5s	0.29	2.2

Table 2. Measured frequency of the first and second structural modes of the four turbine models.



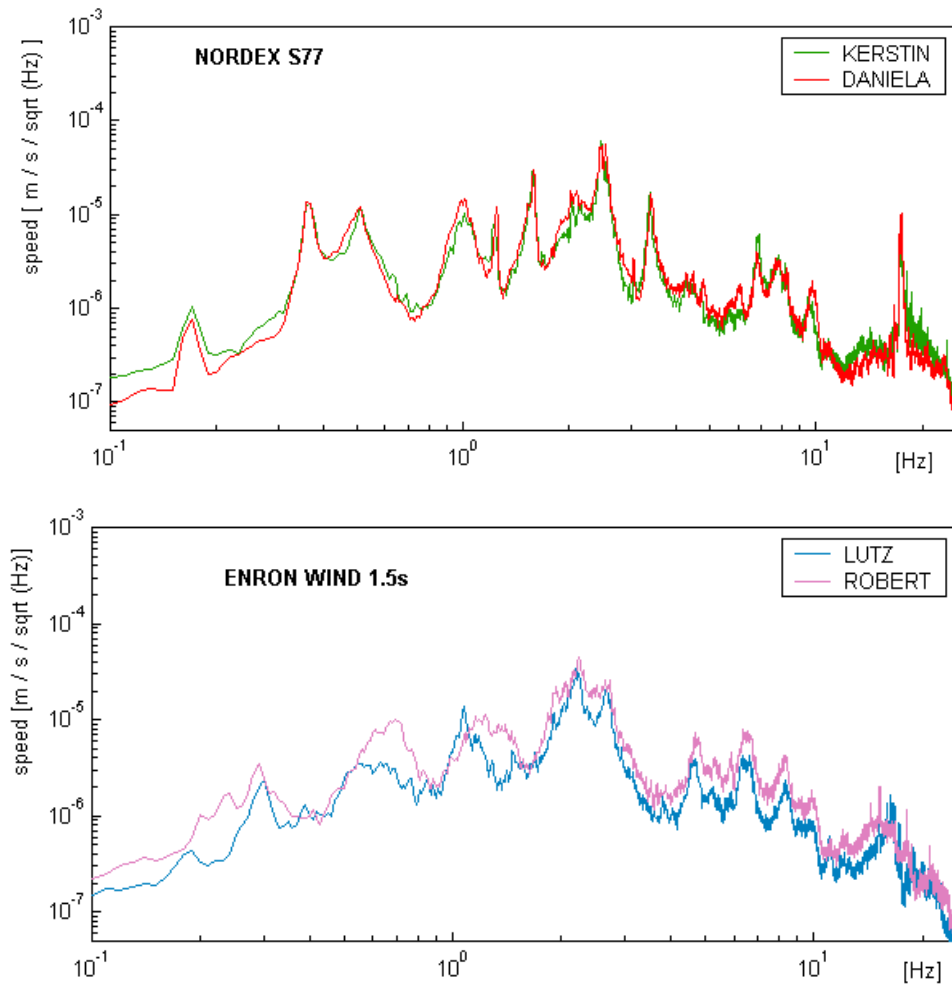


Figure 5. Amplitude of seismic vibration of turbines basement. Three turbine models are compared.

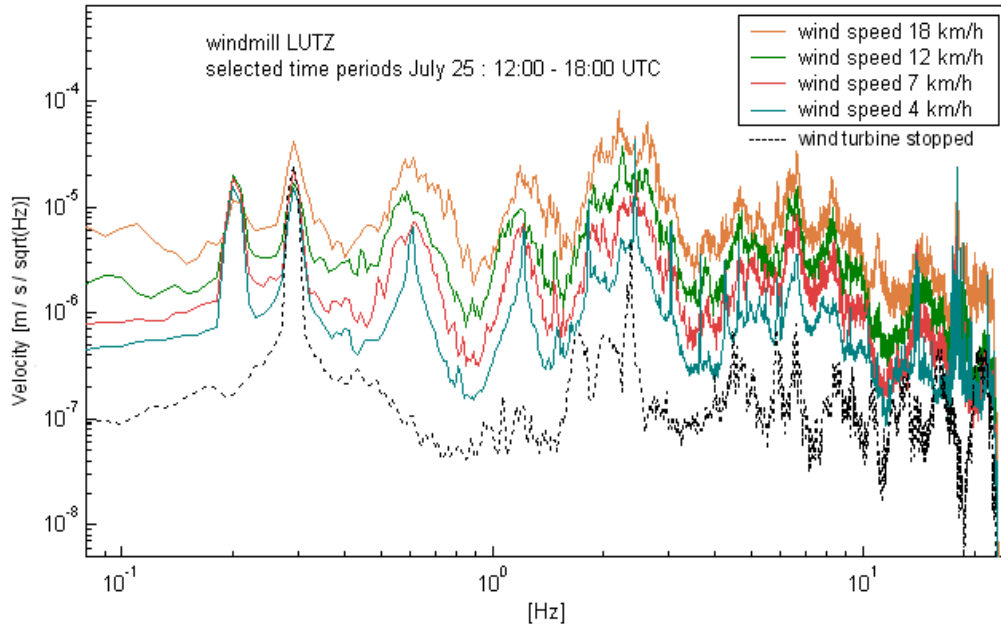


Figure 6. Solid lines are seismic amplitude spectra measured at Lutz base platform in different wind speed conditions; the dotted line is a measurement taken while the turbine was stopped. Quoted wind speeds are measured at soil level.

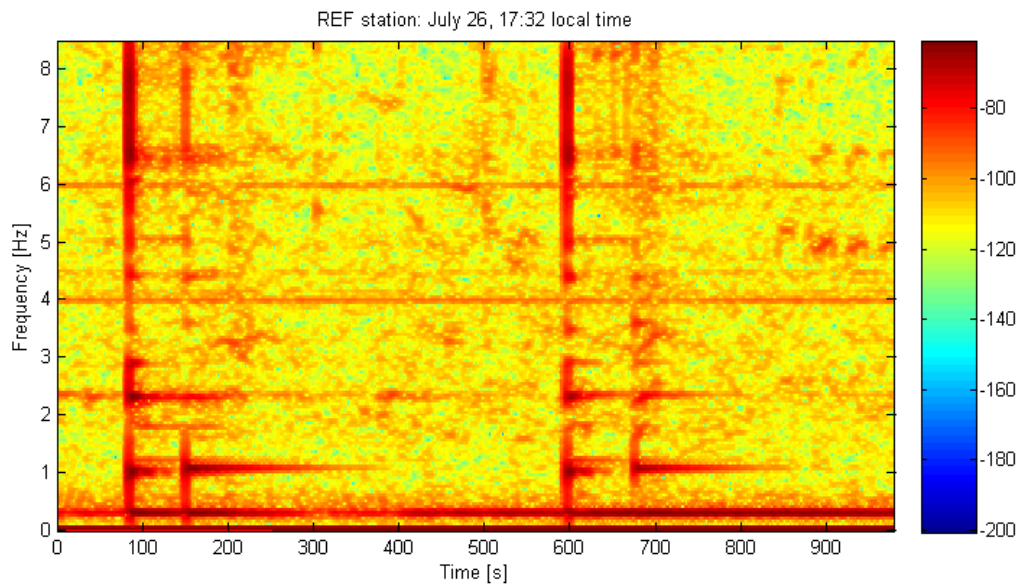


Figure 7. Spectrogram of a 15minutes seismic record at the Lutz basement. Temporary increases of seismic amplitude correspond to re-orientation of the turbine nacelle while the blades were stopped .

### 3. Characteristics of the seismic wave-field from turbines

It is expected that turbines vibrations transmit to the soil through basements and generate persistent seismic surface wave travelling to some distance from the wind-park. A method to detect and study this seismic wave-field, particularly in conditions of elevated background noise, is that of coincidence measurements with an array of seismometers.

We used two tri-axial seismometers, GPS synchronized and aligned. We left one seismometer permanently positioned at Lutz basement platform; while we moved the other one to 13 different out-field sites at variable distances, up to 5km away. A map of recording sites is shown in Figure 3. Three tri-axial seismometer permanently located on the floor of each GEO experimental building were also part of our seismic array.

At least 8 hours of continuous recording was taken at each site. The two most distant sites are located 3km and 5km away and there the seismometer was left recording over-night to catch more quiet times. Most sites are actually in the “near-field” with respect to the wind-park. This was dictated by the need to investigate on the noise produced at the GEO site, and also by the fact that it was not possible to find suited measurement sites, sufficiently distant from roads and houses, at farther distance from the wind-park.

The computation of coherence between the seismic signal at Lutz platform and the signal at out-field stations permitted us to track and study the seismic wave of this particular turbine.

Figure 8 compares horizontal and vertical seismic spectra recorded at Lutz and at increasing distances from it. Figure 9 shows spectral coherences between the seismic record at Lutz and at distant stations. Shown data records were taken with not too different wind conditions, wind speeds at soil ranging from 7 km/h to 11 km/h. For more distant stations (B2 and B3) night-time data are used, because day-time records are dominated by anthropogenic noise from other sources. Seismic records at the two most distant stations (3km and 5km) are dominated by anthropogenic noise also at night-times.

Below 1 Hz all spectra show a persistent seismic peak at 0.3 Hz (Figure 8), which happen to correspond to the frequency of the turbines first structural mode. Between 2Hz and 10Hz the stacked spectra give evidence of a seismic noise component whose amplitude gradually decreases with distance, and which is still detectable at 2 km from the turbines (Figure 8). This noise component is characterized by intense spectral peaks, which reasonably well associate to turbines frequencies. At these peaks, significant coherence is measured between the out-field stations and the vibrations of Lutz platform, this coherence decreases with distance from Lutz (Figure 9). Instead, quite surprising, no coherence is found in correspondence to the intense 0.3Hz spectral component (Figure 9).

The 2-10Hz seismic noise component from the turbines is sensed by the seismometers inside GEO-600 buildings. This is demonstrated by a study shown in Figure 10: comparing seismic spectra recorded during a few night-time periods when the turbines were stopped and when turbines were running. A clear excess (about a factor 5 above background) is detected between 2 and 10 Hz. Typical turbine peaks are spotted. During day-times the excess is less evident; it is partially covered by human activities related noise.

The 2-10 Hz seismic noise looks richer in horizontal than vertical components. This is shown in Figure 11, displaying the ratio of horizontal to vertical spectra recorded by station A1, deployed in the soil close to the GEO central building. This is true also for the background noise, recorded when turbines are stopped. In conditions of strong wind the horizontal to vertical ratio is enhanced in correspondence of the frequencies of turbines emission.

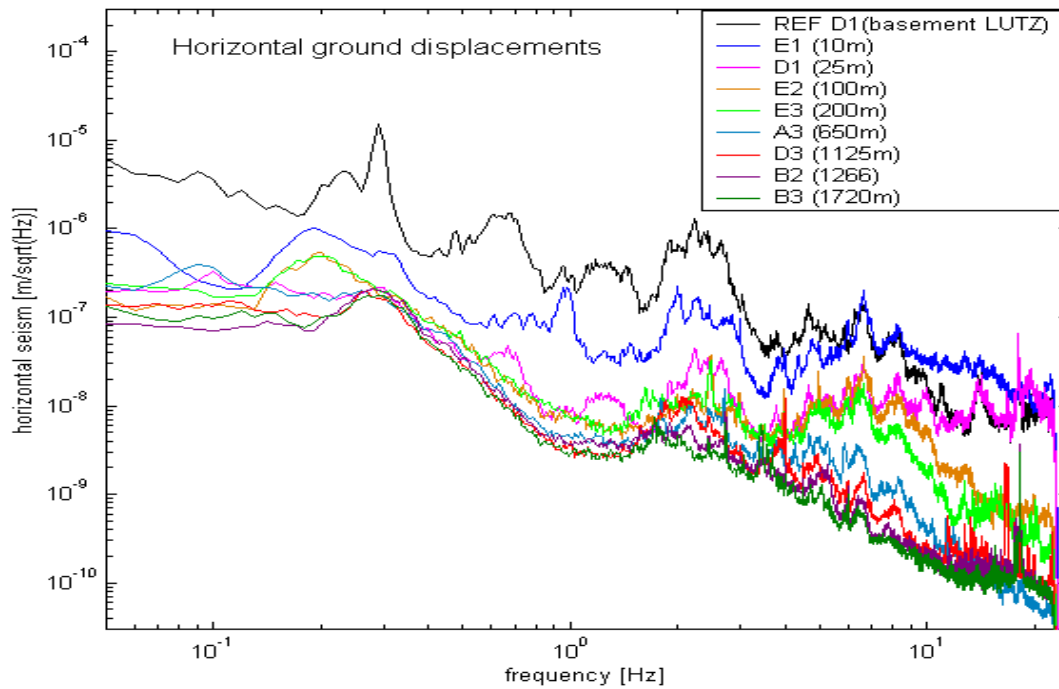
The presence of coherence between Lutz station and the out-field stations (Figure 9) persisting over long periods, points to the existence of a persistent seismic wave in the soil produced by the turbines. The propagation time (and thus the velocity) of this wave can be measured by looking for the maximum of the correlation function between the seismic signal at Lutz and the signals at one out-field station, for different time shifts between the two signals [9,10]. This computation is represented with a “correlogram” plot.

Figure 12 shows correlogram plots which measure the propagation time of the seismic wave between station “REF” at the Lutz platform and station “A1”, located 1130m North-East from REF. The four correlograms in Figure 12 analyze the seismic wave-field in four different frequency bands (2-3Hz, 4-5Hz, 6-7Hz and 8-9Hz). This is done by band-pass filtering the signals before correlating them. The propagation times measured in Figure 12, together with similar ones measured from correlating REF signal with other stations, seem consistent with the hypothesis of a seismic wave propagating in radial direction from Lutz with a particularly slow velocity. We measured:  $v=(450\pm 50)\text{m/s}$  for the 2-4Hz component,  $v=(260\pm 50)\text{m/s}$  for the 4-10Hz component. We thus derive indication of a slowly propagating seismic wave whose speed decreases with frequency. These characteristics, including the fact that the seismic signal is richer in horizontal than vertical components, seem consistent with a shear type of seismic wave (also known as Love waves [11]) travelling in aerated soils as are the agricultural cultivated soils surrounding the Schliekum park and GEO.

We performed a similar correlation analysis for the 0.3Hz seismic component. This is particularly interesting since its frequency coincides with the structural mode of the turbines. The 0.3Hz signals is detected by all out-field stations; it is coherent among all stations, although it is not coherent with the seismic signal at Lutz. The result of the correlation analysis is that: (i) the 0.3Hz signal is quite stable (both in frequency and amplitude) and persistent over the four days; (ii) it is associated to a seismic wave field which travels from the North-East direction ( $48^\circ\pm 4^\circ$  N, i.e. opposite to the wind park) with velocity =  $800\pm 50\text{m/s}$ . Indeed, the dominant 0.3Hz signal detected by out-field stations is not originating from the Schliekum wind park. We initially

hypothesized the 0.3Hz might be the 1<sup>st</sup> harmonic of oceanic microseism (whose typical fundamental frequency is 0.1÷0.15 Hz [12]).

A subsequent study revealed that the typical oceanic microseismic signal at GEO has a dominant 150mHz component, and propagates from North, with a velocity of the order of 6 km/s. One alternative hypothesis is that the observed 0.3Hz peak originates from another wind park. The closest one in the North-East direction from GEO is located about 4.5 km far and counts 10 turbines. This wind park is older than the Schliekum and might have more unbalanced and noisy turbines. However, the origin of the 0.3Hz seismic component, although interesting, remains unknown.



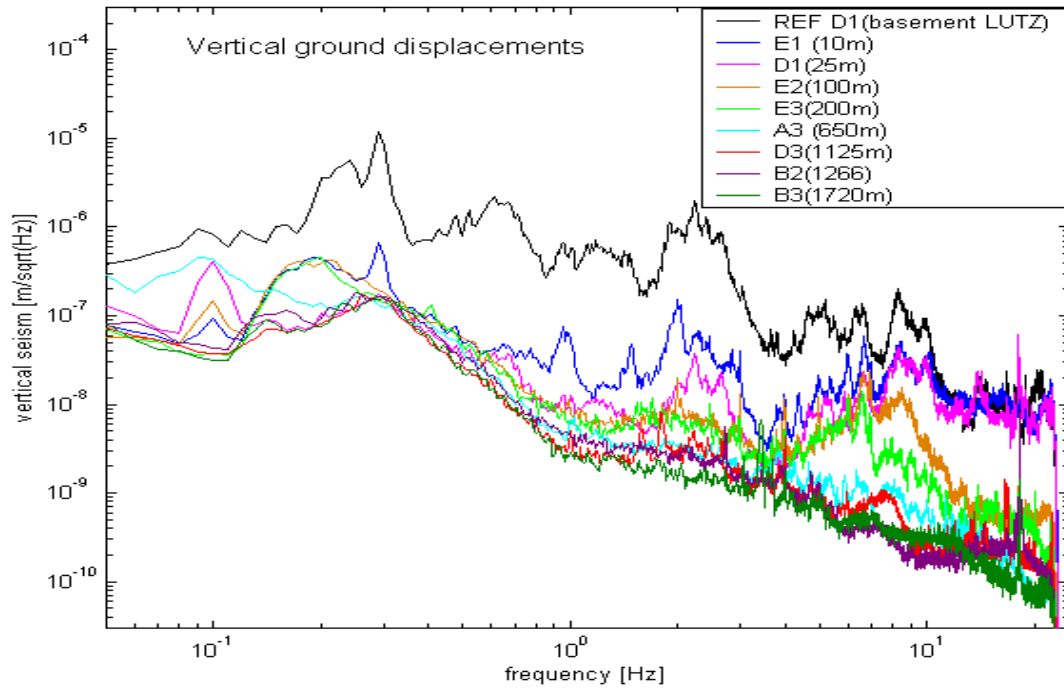
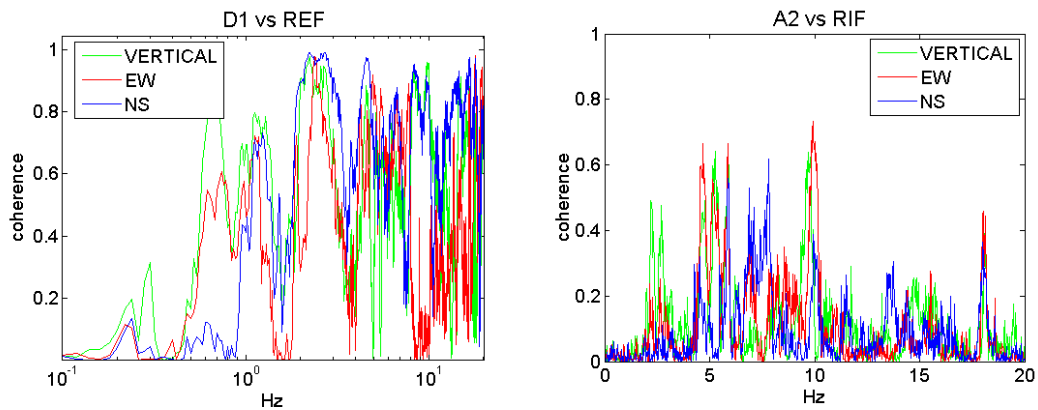


Figure 8. Displacement seismic spectra at Lutz platform (black), and at increasing distance towards GEO-600 and beyond (in colors). Each spectrum is averaged over about one hour. Top plot shows the average soil displacement noise measured along two orthogonal horizontal directions; Bottom plot shows soil vertical displacements.



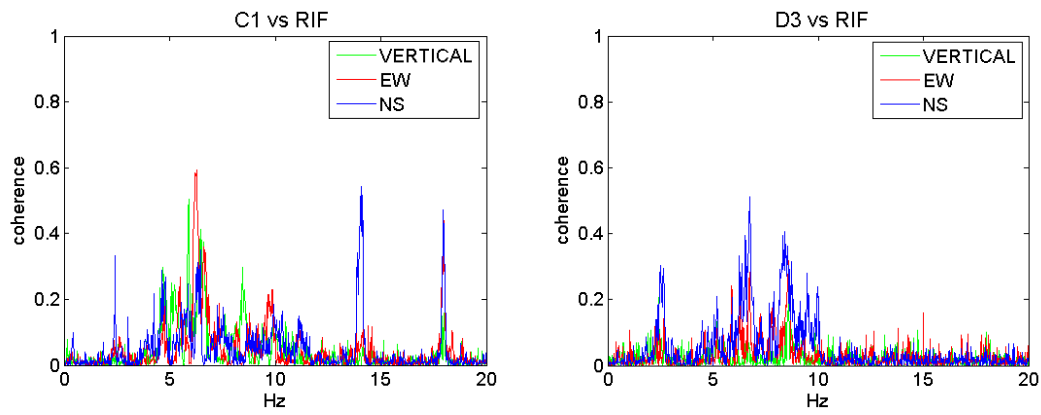


Figure 9. Coherence between the seismic signals at Lutz and at four locations at increasing distance from it: 25m, 300m, 630m and 1130m (clock-wise from top-left). The first plot is displayed with a logarithmic x-axis, to evidence the absence of coherence at the 0.3 Hz peak.

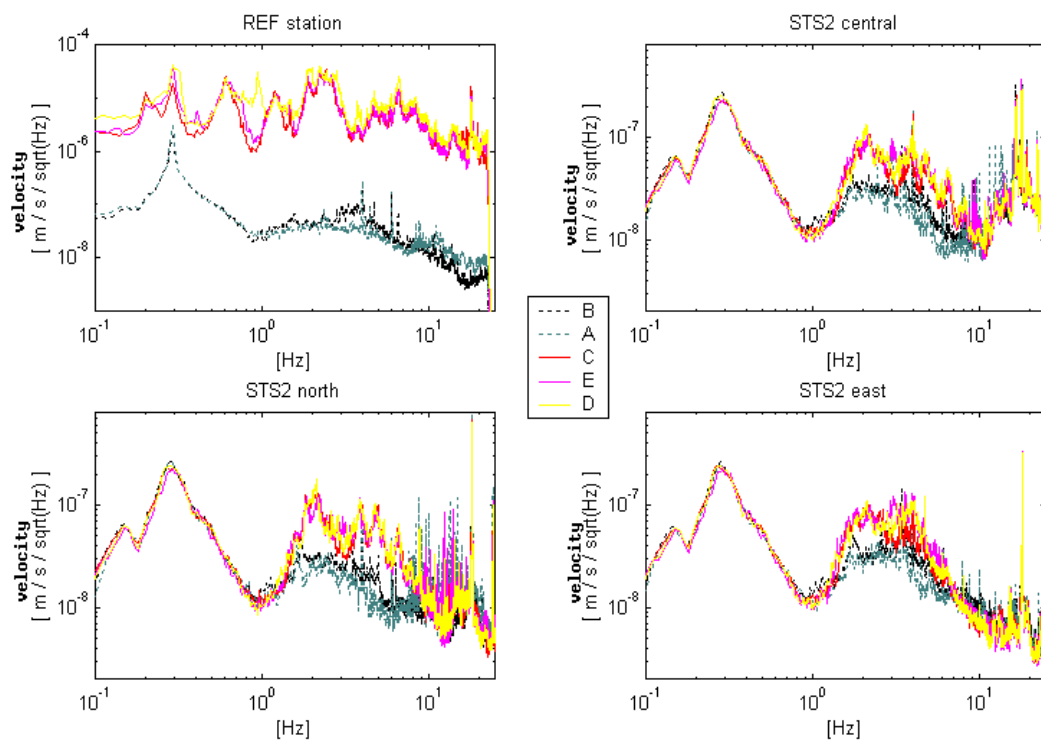


Figure 10. Seismic spectra at windmill Lutz and three GEO buildings corresponding to two night-time periods with all turbines stopped (A,B) and three night-time periods with turbines running (C,D,E).

### H/V Spectral Ratio: Station A01

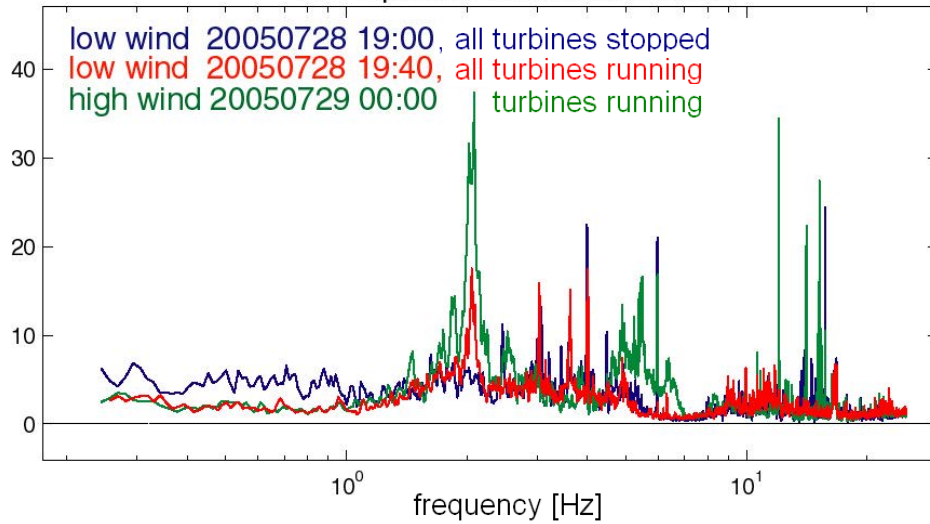


Figure 11. Ratio of horizontal and vertical seismic spectra measured by station A1. Three conditions are compared: all turbines stopped (blue), all turbines running with low wind (red) and all running with strong wind (green).

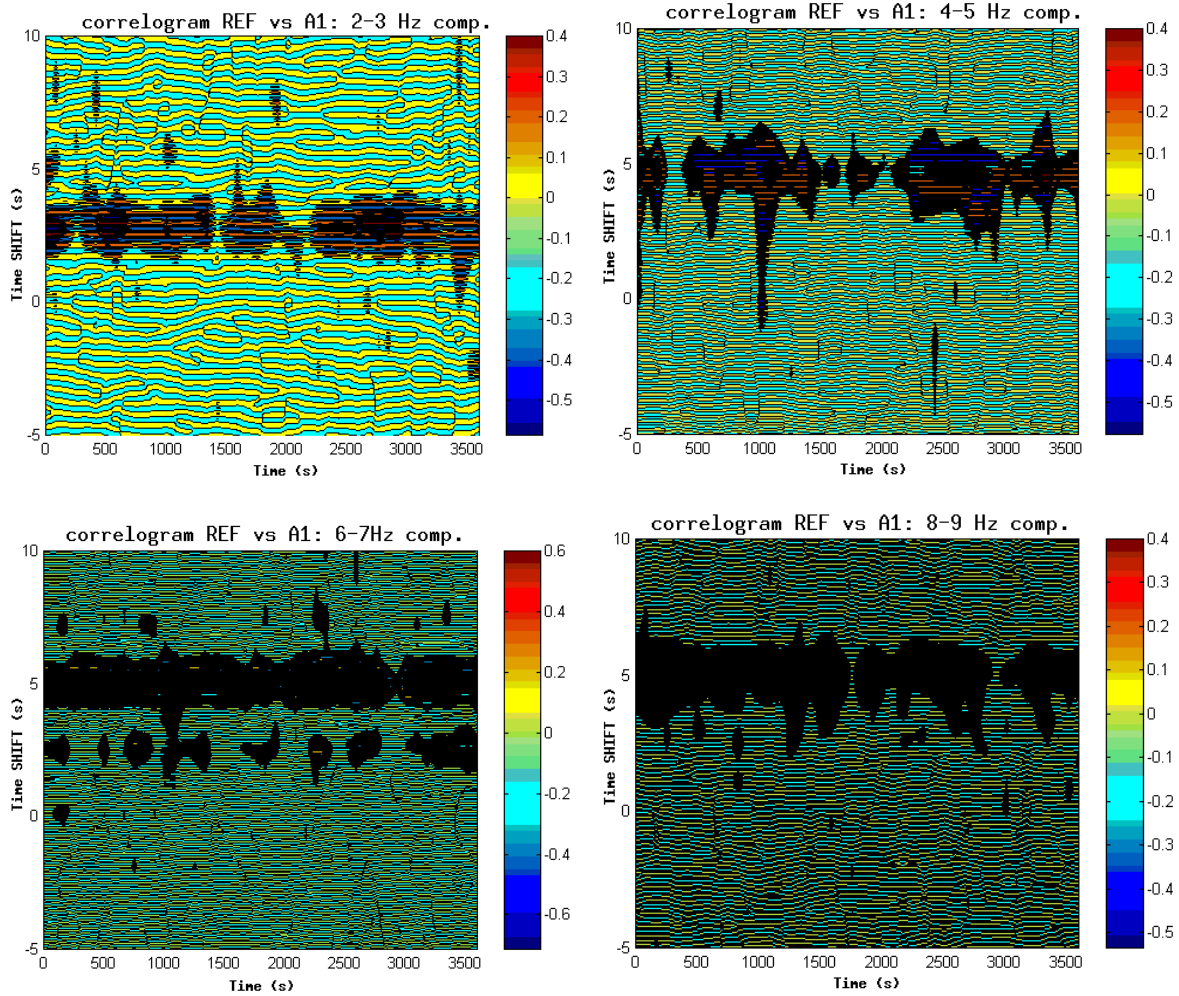


Figure 12. Correlation analysis of seismic tracks recorded by stations REF and A1 (1130m away). Signals were first band-pass filtered. The four correlogram plots are produced correlating the REF and A1 signals filtered in four different frequency bands (clock-wise from upper left: 2-3Hz, 4-5Hz, 6-7Hz and 8-9Hz). In each plot the dark region identifies the maximum of the correlation function of the two signals as function of time. For the upper left plot, the maximum correlation occurs when the REF signal is delayed by +2.5s with respect to REF. This measured delay is constant as function of time (over 1 hour). This indicate for a persistent wave-field propagating from REF to A1 with a velocity of 450 m/s. Similar considerations apply to the other plots.

#### 4. A model for seismic wave absorption

We used coincident records to measure the attenuation of the seismic wave-field as a function of distance from the wind park. As discussed in Section 3, the measured wave-field does not contain well identified spectral peaks which could be tracked in all recording sites. On the other hand, both the coherence studies (Figure 9) and the comparison of distant seismic spectra (Figure 8), indicate that the seismic wave field from the turbines is richer in frequency components between 2Hz and 10Hz. Thus, we measured the attenuation of this composite wave-form. The advantage is that we maximize the signal to noise ratio by including all the most intense signal components. The drawback is that we average over a possible frequency dependence of the absorption law.

We proceeded by selecting, for each measuring site, about 4 hours of clean data, having excluded periods with turbine stopped or transients (transient events, like those caused by passage of cars, are identified with visual inspection of the data in the time frequency domain by means of spectrogram plots). We then extracted the wave form component by filtering the data with one Butterworth band-pass filter with 2Hz and 10Hz cut-offs. We did the same for the coincident recordings of the REF station and of the far station. We then computed the amplitude root mean square (RMS) of both filtered signal. We analyzed separately horizontal and vertical components (we averaged the two orthogonal NS and EW components to one effective horizontal component). We then computed the ratio of the RMS at the far station over that of REF station. In the reasonable hypothesis that the amplitude of seismic emission of all Schliekum turbines is affected by wind speed in the same way, this operation factors-out the effect of variations of the wind speed during measurements. Finally, we normalized the RMS ratios to the horizontal seismic RMS value recorded at station E1 (Figure 3), which was buried in the ground close to Lutz foundation<sup>1</sup>.

The normalized RMS ratios are plot in Figure 13, separately for the horizontal and vertical components. We find indication that the horizontal and vertical components

---

<sup>1</sup> The seismic signal measured onto the turbine platform appears not to be a good reference for measuring attenuations, since the basement can amplify seismic vibrations. Qualitatively this effect can be observed in Figure 8, comparing the seismic spectrum measured by the REF station on the concrete with spectra measured by station E1 deployed in the soil but very close to the basement edge. It seems that vertical vibrations are amplified by about a factor two more than horizontal ones. In addition, the basement seems to enhance low frequencies up to 5-6 Hz.

of the seismic wave-field from the wind park follow the same attenuation law, although the amplitude of the vertical component is about a factor 1.75 smaller than the horizontal component at any distance from the turbines (this is consistent with measurements discussed in Section 3). At distances greater than 1.5km we note a saturation effect. This indicates that the turbines RMS noise is overcome and masked by anthropogenic noise from other sources.

A simple model for the propagation of a seismic wave from a surface source, as for example the wind turbine, assumes that the seismic energy is radiated uniformly from the source along a circular wave-front. The attenuation of the wave amplitude with distance is then described by the formula [11]:

$$(1) \quad A_R = A_r \frac{\sqrt{r}}{\sqrt{R}} \cdot \exp\left(\frac{-\pi \cdot f \cdot (R-r)}{Q \cdot v}\right)$$

Where:  $R$  is the distance from source where the signal amplitude is  $A_R$ ,  $r$  is the distance of a reference nearer ( $r \ll R$ ) location where the signal amplitude is  $A_r$ . The exponential term accounts for the energy dissipation in the soil. This is parameterized with a quality factor  $Q$  which ...,  $v$  is the wave velocity and  $\omega=2\pi f$  is the wave frequency.

We applied this model to the multiple incoherent sources of the Schliekum wind park. We computed the total seismic ( $A_j$ ) amplitude at one measuring location " $j$ " as the quadratic sum of the seismic amplitude at " $j$ " of the seismic waves from each turbine,  $A_{i,j}$  (the index " $i$ " identifies the turbine: " $i$ "=1,...8):

$$(2) \quad A_j = \sqrt{\sum_i A_{i,j}^2}$$

$$(3) \quad A_{i,j} = \frac{K}{\sqrt{R_{i,j}}} \cdot P_i \cdot \exp\left(\frac{-\pi \cdot f \cdot R_{i,j}}{Q \cdot v}\right)$$

$$(4) \quad K = A_0 \sqrt{r_0} \frac{1}{P_0} \exp\left(\frac{\pi \cdot f \cdot r_0}{Q \cdot v}\right)$$

Where:  $R_{i,j}$  is the distance of turbine " $i$ " from location " $j$ ",  $P_i$  is the power of turbine " $i$ " (see footnote <sup>2</sup>), and  $K$  is a constant factor which accounts for the seismic amplitude measured at one reference distance from one reference turbine.

The parameters we use in the model are the following:

- $f = 6$  Hz, is the central frequency of the chosen RMS frequency range;
- $v = 310$  m/s, is the weighted average of the measured velocity (Section 2);

---

<sup>2</sup> Our measurements indicate the turbine seismic amplitude is proportional to wind speed (Section 2 and Figure 6), on the other hand, turbines power is approximately proportional to wind speed in the rated working range. We thus assume seismic amplitude to be proportional to turbines power.

- According to literature [11] a value of  $Q$  in the range 20 to 100 is reasonable for a sandy clay type of soil. We tested our model with values of  $Q \cdot v = 6000$ , 15000, and 30000.

The hypotheses of uniform radiation and of linear superposition indeed are not strictly valid in the near field of the sources. In fact, the presence of obstacles (buildings, other turbines) or soil non-homogeneities on the wave-field path can cause local build-ups or dilutions of seismic energy. Therefore we do expect the model to have some degree of uncertainty when applied to measurements done in the vicinity of the turbines, at distances smaller than a few times the signal wavelength (in our case  $\lambda \approx 50\text{m}$ ).

Figure 14 compares the measured horizontal attenuation to the prediction of the attenuation models. Values of  $Q \cdot v$  in the range 15000 to 30000 appear to adequately reproduce the data. This poor estimate suffers mainly of the fact that we could not perform significant measurements beyond 2 km from the windmills, because there the windmills signal was overcome by anthropogenic noise of different origin.

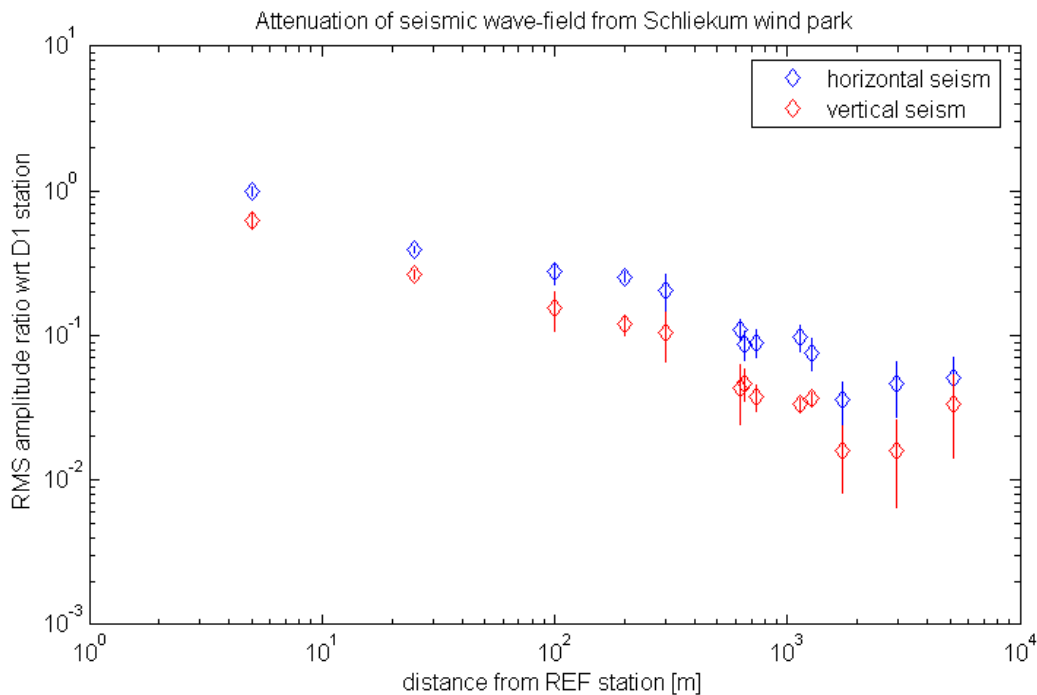


Figure 13. Attenuation of the amplitude of the seismic wave-field from the Schliekum wind turbines: horizontal (blue) and vertical (red) components. The plotted dots are the ratio of the 2-10Hz RMS amplitude measured at out-field stations (A1 to D3), corrected by wind speed, to the horizontal RMS measured at station E1 (5m). On the horizontal axis is reported the distance of out-field stations from REF station on Lutz platform. Each RMS is computed over four hours of data (cleaned from transients)

and turbines off periods) at 100s steps. The bars show the statistical uncertainty associated to the variance of RMS values.

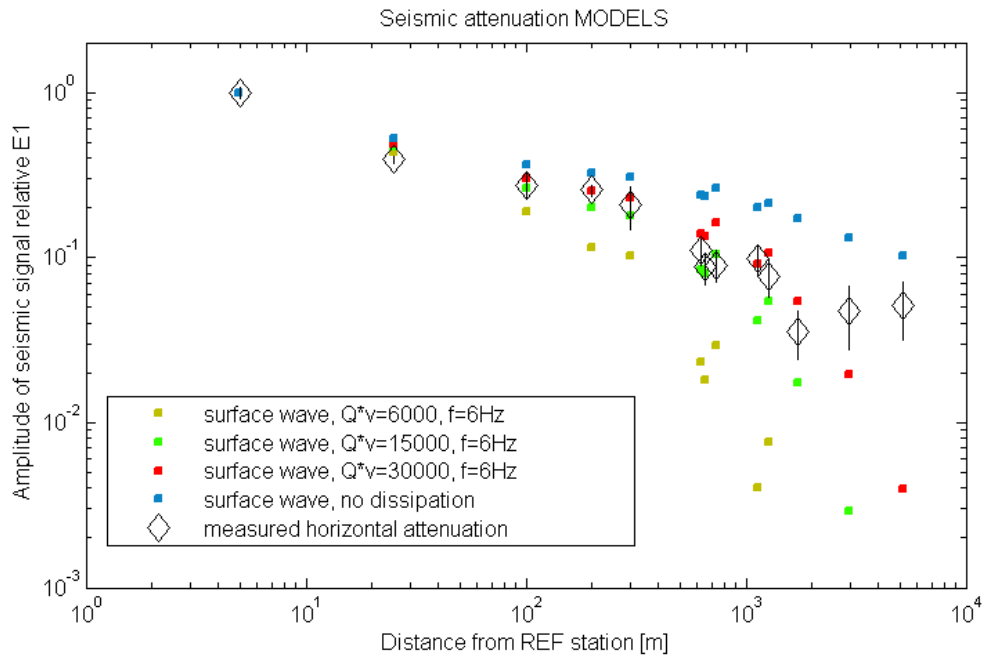


Figure 14. The measured horizontal attenuation as function of distance (blue diamonds) is compared to the predictions of the attenuation model. Squares of different colours correspond to four different values of the  $Q \cdot v$  parameter, or, assumed a velocity  $v=300 \text{ m/s}$ , four different values of the soil attenuation factor:  $Q=20, 50, 100$ . Also the ideal case of a non-dissipative soil is represented.

## 5. Prediction of seismic noise at VIRGO by “il Faldo” wind park project.

The final goal of our study is to derive an estimate of the seismic disturbance (RMS noise level and spectral composition) produced at the VIRGO site from the wind park “il Faldo” proposed for construction in the vicinity of the site. Figure 15 shows the proposed layout of “il Faldo” composed by 9 turbines, Enercon E82, 2.0MW [13]. The turbines are located approximately S-W of VIRGO at distances between 3 and 4.5 km from the (closest) VIRGO West experimental building.

We used the model described in Section 5, with the following assumptions:

- (1) VIRGO and GEO soils have similar transmission properties for mechanical waves, so that the attenuation model we derived for GEO reasonably applies to VIRGO. This assumption is supported by the similar morphology of soils (sandy clay), and by the fact that the velocity of propagation of 2-4Hz surface seismic waves measured at GEO (Section 3) and at VIRGO [14] are similar.
- (2) We assume similar characteristics of the seismic emissions by Schliekum and “il Faldo” wind turbines. We indeed expect the coarse features of the signal spectral composition to depend mainly on the blades rotation frequency and the turbines structural parameters, which are similar for Schliekum and “il Faldo” ones. On the other hand, we expect that the relative amplitude of the

frequency components transmitted to the soil would depend mainly on the characteristics of the turbine foundations, which we assume similar.

Thus, we used formula (2), (3) and (4) (Section 4) with the following settings:

- we defined locations “ $j$ ” where to evaluate the seismic noise of “il Faldo” (black dots in Figure 15);
- we inserted in “ $r_{ij}$ ” the geometrical layout of “il Faldo” and turbines power  $P_i$ ;
- being interested in a conservative estimate of the noise produced, we adopted, within the  $Qv$  range determined above, the value  $Qv=30000$ , corresponding to a less dissipating type of soil (given a wave speed  $v\approx 300\text{m/s}$ , this corresponds to a soil quality factor  $Q=100$ ),
- we adopted the same average frequency  $f=6\text{Hz}$ , and RMS range  $2\div 10\text{Hz}$ ;
- we adopted as reference seismic RMS amplitude ( $A_0$ ) the seismic noise produced by turbine Lutz ( $P_0=1.5\text{MW}$ ) measured by station E1 in conditions of an average wind speed of  $8\text{ km/h}$  (measured at soil level).

Figure 16 shows the predicted RMS seismic amplitude ( $2\div 10\text{Hz}$ ) produced by “il Faldo” at increasing distances towards VIRGO, and its expected excursion associated to variations of wind speed in the range  $4$  to  $25\text{ km/h}$  (at soil level). The expected noise is compared to the typical values of  $2\div 10\text{Hz}$  RMS environmental seismic noise measured at the VIRGO site. In this frequency range, the site seismicity is dominated during working hours by the noise produced by local traffic and follows a daily amplitude variation of about a factor 6 (90% C.L.) [15,14].

The result is that the wind park would produce an observable effect at the VIRGO West station (North and Central stations instead would be substantially unaffected). The increase of seismic noise at the West station would be within the range of RMS variations due to other anthropogenic sources (Figure 16). However, in order to correctly evaluate the impact of the noise on the VIRGO interferometer, we have to consider the spectral composition of the noise. In fact, seismic peaks in correspondence of the mechanical resonances of the mirror suspensions can excite high- $Q$  modes and make the system unstable.

Figure 17 gives an idea of the spectral amplitude of the seismic signal from the “il Faldo” turbines that would be measured at the VIRGO West station. The prediction has been obtained using the amplitude spectrum recorded at E1 and rescaling it to the value of predicted RMS at the West station. An upper limit is computed increasing this spectral noise by a factor three to account for wind speeds up to  $25\text{ km/h}$  (soil level). We compare these predictions to the spectral amplitude of the typical seismic noise from (other) environmental sources measured at the VIRGO site. We find that seismic spectral peaks from the “il Faldo” turbines would significantly exceed the present seismic noise, in conditions of moderate-high wind, but only at the Virgo West experimental hall which is the closest ( $\approx 3\text{km}$ ) to the wind park.

Although the precise frequency position of the seismic peaks between 2 and 10 Hz might be different for the “Il Faldo” windmills, our projection indicate a significant disturbance. The frequency region above 4 Hz appears to be the most exposed. At present the day-time increase of seismic noise in the 2-10 Hz range is due to transient signals associated to road traffic [14,15]. Seismic noise from turbines would be instead of a persistent nature, thus more critical for the VIRGO detector, being capable of exciting mirror suspensions resonances.

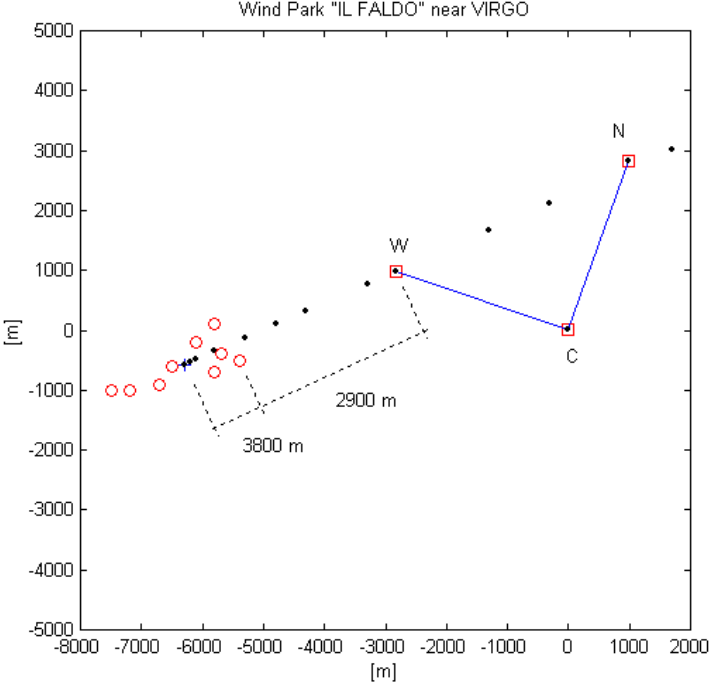


Figure 15. Proposed layout of “il Faldo” wind park. Red circles indicate turbines. Also depicted is the position of VIRGO experimental Buildings (C=central, W=West, N=North). Black dots mark the points where the model prediction was evaluated.

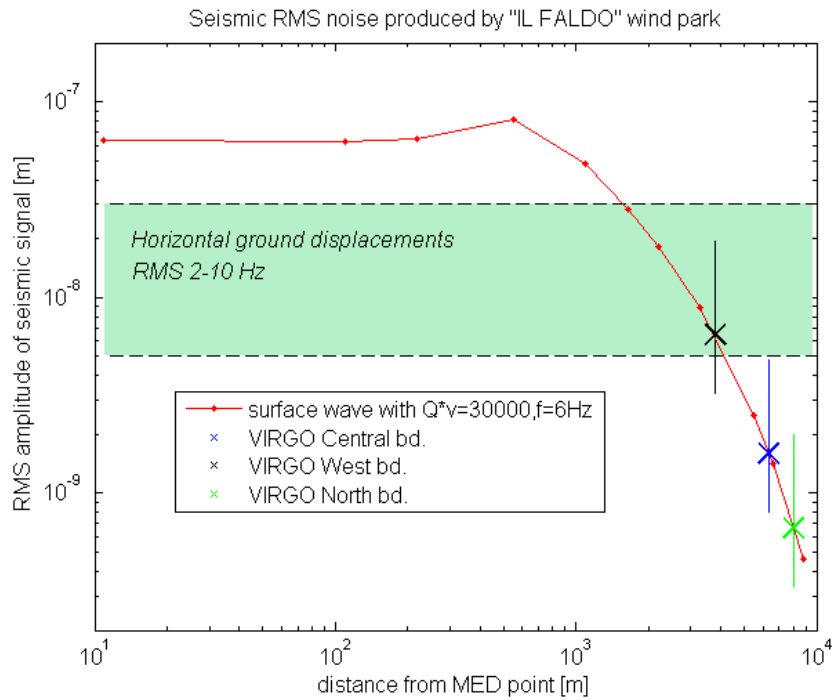


Figure 16. Prediction of seismic RMS displacement (2-10 Hz) produced by "Il Faldo" wind turbines at increasing distances towards VIRGO. Distances are measured for convenience from the geometrical barycentre of the turbines position (MED). The green rectangle delimits the range of RMS seismic noise variation measured at the Virgo site. Crosses mark the RMS noise expectation at VIRGO buildings for a typical average wind speed of 8 km/h. Vertical bars represent the variation in RMS noise we expect associated to variations of wind speed between 4 and 25 km/h. These are wind speed values measured at soil level, we assume they correspond to the minimum and maximum wind speed values of typical operational range of turbines.

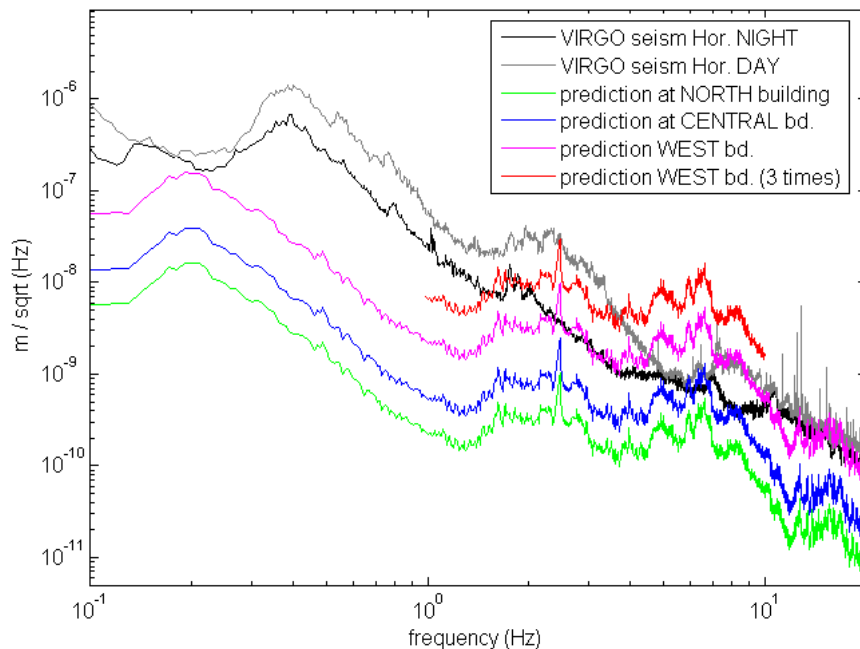


Figure 17. Black and gray curves are typical seismic noise displacement spectra at the VIRGO site, recorded during night-times (black) and day-times (gray). These are compared to the predicted spectral noise produced by the “il Faldo” turbines at the location of the VIRGO experimental buildings (in colors). The parameters used for the attenuation model are the same used in Figure 16. Magenta, blue and green curves are computed for an average wind speed of 8 km/h (measured at soil level), which we assume corresponds to the mid-range wind speed of turbines operation. The red curve shows the expected noise level at VIRGO West building in case of a three times stronger wind, which we assume corresponds to the upper limit of the operational range of turbines.

## Conclusions

We studied the seismic wave-field generated by one wind park located in a not particularly quiet seismic area (25 km from the city of Hannover) on a cultivated soil and composed of lime and sand sediments (thus particularly seismically dissipative-type of soil).

We find that the seismic wave-field is particularly rich in the 2 to 10 Hz frequency components, which correspond to functional frequencies of the turbines. The surface seismic wave has the characteristics of a Love wave with a dominant horizontal component. The velocity of propagation is particularly slow, 500÷250 m/s, with evidence of dispersive effects (higher components travel slower). A qualitative indication is that at about 2km distance from the park the wave-field amplitude reduces to a level comparable to the variation of the anthropogenic seismic noise.

A simple model of incoherent superposition of uniformly radiated surface seismic waves from the single turbines seems to reproduce the measured seismic wave-field attenuation with distance, for values of the  $Q \cdot v$  parameter in the range 15000÷30000. The uncertainty of the model predictions is however large because we applied it to measurements in the near-field of the wind park.

Based on this model we expect that a similar wind park proposed for construction in the vicinity of the VIRGO detector in Italy, would produce a disturbance significantly above of the typical RMS variation of the site seismicity, up to about 4 km distance.

Based on this result and conservatively accounting for the model uncertainty, we set a minimum “distance of respect” of 6km from each of the VIRGO buildings for the installation of the wind park, counting 9 turbines of 2MW. This distance scales with the square root of the number of turbines and linearly with the turbines power.

## References

- [1] Saulson P.R (1994) “Interferometric gravitational wave detectors”, World Scientific.
- [2] VIRGO: <http://www.ego-gw.it/virgodescription/> ; GEO: <http://geo600.aei.mpg.de/>; LIGO: <http://www.ligo.caltech.edu/>; TAMA: <http://tamago.mtk.nao.ac.jp/>.

- [3] Schofield R (2001), "Seismic Measurements at the Stateline Wind Project", LIGO T020104-00-Z.
- [4] Style P (2005) "A Detailed Study of the Propagation and Modelling of the Effects of Low Frequency Seismic Vibration and Infrasound from Wind Turbines", WTN 1<sup>st</sup> International Meeting, Berlin, October 2005.
- [5] Fiori I, presentation at [2nd ILIAS-GW Annual Meeting](#), Palma de Mallorca, October 2005.
- [6] NORDEX <http://www.nordex-online.com/en/products-services/wind-turbines/n90-23-mw/>; ex-ENERCON: <http://www.gepower.com/home/index.htm>.
- [7] Peterson J (1993) "Observations and modeling of background seismic noise", U.S. Geological Survey Tech. Rept., 93-322, 1-95.
- [8] Schaumann P, Seidel M (2000) "Einschwingverhalten von Windenergieanlagen", Berechnungen und Messungen Hannover.
- [9] Marchetti E, Mazzoni M, Ripepe M (2002) "Low frequency seismic wave-field array analysis at Virgo", VIRGO NOT-FIR-1390-220.
- [10] Justice J H, et al. (1985) "Array Signal Processing", S. Haykin Editor, Prentice-hall, pp. 432.
- [11] Lay T, Wallace T.C (1995) "Modern Global Seismology", Academic Press.
- [12] Braun T, Ripepe M et al (1998) "On the origin of the long-period tremor recorded at Stromboli Volcano", Annali di Geofisica, vol.39 pp 311-326.
- [13] <http://www.enercon.de/>.
- [14] Fiori I, Holloway L, Paoletti F (2003) "Study of the 1 to 4 Hz seism at VIRGO", VIRGO NOT-FIR-1390-251.
- [15] Fiori I (2003) "Properties of seismic noise at the Virgo site", *Class. Quantum Grav.* **21** S433-S440.